Feasibility Study of X-Ray Fluorescence for Analysis of Welding and Brazing Fumes

Thomas P. Carsey, Ph.D.

Public Health Service
Center for Disease Control
National Institute for Occupational Safety and Health
Inorganic Methods Development Section
Cincinnati, Ohio

November, 1980

EXECUTIVE SUMMARY

This report covers work performed at NIOSH during FY79-80 to determine the feasibility of the technique of X-ray fluorescence (XRF) for the analysis of welding and brazing fumes in air. The investigation required development of welding facilities and sampling systems, experience in X-ray fluorescence instrument operation, field sampling, and chemical analysis. It was pursued as a sequence of steps described below:

(1) A sampling device was constructed which permitted uniform, homogeneous deposition of welding or brazing fumes on six standard filter cassettes simultaneously. The device was located above the NIOSH arc welding station.

(2) Fume samples from (1) were examined by electron microscopy and X-ray diffraction in order to assess the particle size and deposition homogeneity, factors known to be important in the XRF technique.

(3) XRF instrument parameters were developed for all elements of interest.

(4) The fume samples from (2) were analyzed by XRF, ashed, and analyzed by atomic absorptions to determine the nature of the concentration - intensity relationships. The samples were also analyzed by inductively-coupled argon plasma emission spectroscopy (ICP).

(5) An XRF standardization method was developed using generated fume samples. Three sets of six filters deposited with low, medium, and high amounts of fume were obtained. Half were ashed and analyzed by AA and ICP, the remaining half used as XRF standards (three each at the three deposition levels).

(6) Field samples were obtained at three Cincinnati welding shops. These samples were quantitatively analyzed by XRF according to the standards developed in (5). Subsequently, they were ashed and checked by analysis by AA and ICP.

(7) This data was analyzed statistically to provide accuracy and precision data to substantiate the degree of feasibility of the technique.

(8) The XRF technique was shown to be feasible for fume analysis; however, a more adequate standardization procedure is needed before a NIOSH method can be promulgated.

Table of Contents

Page	Item
4	1 Introduction
5	2 Characterization of Welding and Brazing Fumes
5	2.1 Generation and Sampling
5	2.1.1 Generation Equipment
5	2.1.2 Sampling Equipment
6	2.2 Fume Characteristics
6	2.2.1 Deposition Characteristics
6	2.2.2 Electron Microscopy Analysis
7	2.2.3 X-Ray Diffraction Analysis
8	3 Instrument Paramters
8	3.1 Qualitatiave Analysis of Generated Samples
8	3.2 Instrument Parameters
9	3.3 Deposition - Intensity Relationships
10	3.3.1 AA vs. ICP Results
11	3.3.2 Loading Limits
11	3.3.3 Concentration - Intensity Relationships
12	3.4 Summary
13	4 Analysis of Field Samples
13	4.1 Qualitative Analysis
14	4.2 Instrument Characteristics
14	4.2.1 Standard Curves
14	4.2.2 Minimum Detection Limits
15	4.3 Quantatitive Analysis
15	4.3.1 Deposition - Intensity Plots
15	4.3.2 Numerical Results
16	4.3.3 Individual Elements
17	4.3.4 Absorption Coefficients
19	4.4 Other Standardization Techniques
19	4.4.1 Multiple-Drop Method
19	4.4.2 Filter Deposition Method
20	4.5 Instrument Difficulties
20	5 Conclusions
20	6 Acknowledgements
21	References
23	Figures
45	Tables
59	Appendices

FEASIBILITY STUDY OF X-RAY FLUORESCENCE FOR ANALYSIS OF WELDING AND BRAZING FUMES

1. Introduction

The need for a rapid, multielement analytical method for the analysis of metal fumes produced by welding and brazing operations has increased as the toxic effects of these substances have become more evident [1].

The purpose of this study was to determine the feasibility of using the technique of wavelength-dispersive X-ray fluorescence (XRF) for such analysis. This technique offers the advantages of (1) minimum or zero sample preparation; (2) rapid analysis of any solid element with atomic number greater than 11; and (3) the nondestructive nature of the analysis allowing for subsequent chemical analysis or permanent storage of the sample. However, because of the lack of experience at NIOSH with this technique, this effort was as a necessary preparatory investigation prior to actual method development.

A feasibility study should accommodate the widest possible range of welding and brazing processs. The most important of these processes, according to the American Welding Societyare shielded metal arc (SMAW or Stick), submerged arc (SAW), gas metal arc (GMAW or MIG), gas tungsten arc (GTAW or TIG), and flux-cored arc welding (FCAW)[2,4]. These processes are described in Figure 1; Table 1 gives the metals commonly associated with each. (An excellent discussion of welding processes is given in reference 3).

Both gases and fumes are produced by welding and brazing processes [5,6]; however, this study is involved only with fume analysis. These fumes are known to contain a number of elements. These elements have been outlined in Table 2 along with levels which have been reported in welding work situations, the TLV values, and the analytical range for the analytical method (atomic absorption) currently recommended (data from reference 6). Thus, a useful analytical method must be capable of analyzing for a large number of elements at the levels observed. The reported minimum detection limits for the XRF technique (Table 2) indicate that the method should be feasible for this analysis.

This study of the applicability of x-ray fluorescence for the analysis of fumes generatd by welding and brazing processes was pursued in the following manner: (1) five non-automated processes and their associated metals were chosen which best represent the current welding industry (Table 3); (2) fume samples from the above process were collected and characterized; (3) XRF analysis, ashing and elemental analysis by AA and ICP were performed on the samples in order to thoroughly investigate the fumes

as they relate to the XRF technique; (4) an XRF standization method would be developed; (5) field samples would be obtained and analyzed to ascertain feasibility of the XRF technique.

2. Characterization of Welding and Brazing Fumes

2.1 Generation and Sampling

2.1.1 Generation Equipment

Welding and brazing fumes were generated at the welding facilities of the NIOSH laboratories. Welding was performed with a Miller Model 330A/BP(2) AC/DC Gas Tungsten-Arc Welding Power Source, with a Spool-Matic II MIG electrode, or Weldco Model M-250 stick welding electrode, or Miller Model M2-1, HH-6 plasma arc power supply. Brazing utilized a Victor Model 100 oxyacetylene welding torch. A description and approximate chemical composition of the materials used in the processes is given in Table 3.

2.1.2 Sampling Equipment

A fume collector was built[7] adjacent to the ventilation hood of the welding station (Figure 2), which consistently provided six filter fume samples with about 6% RSD variation of deposition (based on the XRF intensities of major composition elements). An inlet tube drew air from the ventilation air flow and directed the air into the fume collector. The collector was built in a 6" OD, 38" plexiglass tube. The flow disruptor is 3-3/4" diameter disk located 10-1/4" from the lower end of the tube. The flow straightener is a steel plate containing an array of 1/4" holes, with a brass 1" honeycomb on top, located 7-1/4" from the top of the straightener. The tube cover, eighteen inches above the straightener, holds the main flow outlet and filter.

A vacuum draws air through the collector, past the cassettes, and out through the filter. A second pump aspirates the air sample through the filter cassettes, each cassette having its own flow-limiting orifice (1.0 Lpm). The flow rate was periodically measured to check for unclogged lines.

The fume collector was operated while welding was occurring. Welding took place approximately two feet below the inlet tube of the collector.

The gas metal arc (MIG) process produced considerably less fume than the other processes; consequently, a longer inlet tube was used with this process to increase the collection efficiency.

2.2 Fume Characteristics

Fumes are considered to originate in the high temperature vapors of the welding arc. These temperatures have been estimated to be 1400-3100°C [14]. The molten metal pool is at much lower temperature and is thought to contribute much less to the fume. [11] Metal vapors condense rapidly, passing through a liquid phase (hence their spherical shape) into solid. Although the consumable electrode (and flux, if any) will make up the majority of the fume, [9] it is not wise to predict fume compositions based on electrode composition. Components having high vapor pressure will tend to be concentrated in the fume. Crystallinity is usually low due to the rapid cooling. After a short period of time, agglomeration of the particles will occur. The tendency of each chain to be composed of a particular size of particle suggests a similar chemical and thermal history of the individual particles. Stern [9] has observed a bimodal distribution of fume particles from rutile electrodes which he described as follows: the larger particles arise from the flux and the smaller particles arise from the metal vapor condensate.

2.2.1 Deposition Characteristics

For each fume sample, sampling was done at 1 Lpm on Millipore AAWP (37 mm, 0.8 um) filters (or Nuclepore 0.8 um filters for electron spectroscopy). The arrangement always resulted in an apparently homogeneous deposition, with practically no pileup at the center of the filter. In some cases, a slight concentration of larger, black particles was observed in the center but this appeared to constitute a quite small portion of the mass deposited and, therefore, was not considered significant. In no instance was fume deposition observed on the backup pad, even with quite heavy depositions on the primary filter.

2.2.2 Electron Spectroscopy Analysis

Particle size is a critical parameter in XRF (Reference 15, p. 524). Ideally, the analyte thickness should be such that essentially all exciting and emitting X-rays pass through without absorption. This condition results in a linear intensity versus thickness relationship, and will exist in thin samples up to a depth termed the infinite (or critical) thickness. For

example, for chromium, iron, and nickel, this thickness is about 30-40 um. (Reference 15, p. 624). Thus, fume samples with particle sizes of 1 um are not expected to exhibit particle size effects and none are observed (see below).

An investigation into the physical characteristics of welding fumes was undertaken to determine particle size. Filter samples collected in the fume collector previously described were examined by electron spectroscopy [8] (Figure 3). The deposited fumes show up more clearly on the Nuclepore filter (Figure 3A, B). The main characteristics to be seen are: (1) majority of particles are spheres, less than than 0.15 um in diameter; and (2) agglomeration occurs, especially in the mild steel sample (3B). Examination of the mild steel fumes, stick welding (Figures 3B,C) reveals that the majority of the particles are spheres with two size populations: 0.05-0.10 um, agglomerated (primary fraction); and 0.25-0.5 um non-agglomerated. The stainless steel fumes (stick welding) (Figures 3A, D) are not as heavily agglomerated, and display a more even size distribution of 0.05-0.4 um. The reasons for these differences are not clear; in general the dynamics of welding fume generation are not well understood at this time.)

Millipore filters have no flat surface on which to photograph the fume. However, the same fume characteristics can be observed in Figures 3C, D and Figure 4 as seen on Nuclepore filters. Some larger particles are observed with stainless steel-stick (Figure 4B, 4C), the largest being about 1 um. Agglomeration is not absent on these filters. These samples are heavily loaded, yet it appears that most of the deposit is on the upper portion of each filter. Similar deposition characteristics are observed for all welding processes studied. The particle sizes and distributions observed here are in substantial agreement with literature reports. [9-14]

2.2.3 X-Ray Diffraction Analysis

X-ray diffraction studies have been published for welding fume samples.[11-13] Stainless steel stick welding with AWS E316L electrodes (19% Cr, 12.5% Ni, 2% Mn, 2% Mo, 63.5% Fe) resulted in fumes containing γ-Fe_2O_3 and Mn_2O_4.[12] Kimura, et. al [11] detected NaF and $KCaF_3$ in lime-type electrode welding, and MgO and CaF_2 from fluorspar-base flux-cored electrode welding.

X-ray diffraction analysis (Philips APD Model 3501) of heavily loaded filter samples of fume from each of the processes listed in Table 3 was performed. The analysis was impared by lack of crystallinity of the deposits. Only tentative assignments of the few low-intensity peaks are possible (Figure 5 and Table 4). Flux material was not detected in any of the diffraction patterns.

3. Instrument Parameters

3.1 Qualitative Analysis of Generated Samples

Fume samples of the welding and brazing processes listed in Table 3 were obtained on the welding/sampling station described above. Millipore AAWP (mixed cellulose esters) 37-mm filters were used because of their popularity in industrial hygiene sampling for metals. A flow rate of 1 Lpm was used to insure a homogeneous deposition of the fumes on the filters. Sample depositions at three to five loading levels (determined visually) were obtained with six filter samples at each loading level. One filter out of six was used for electron spectroscopy and X-ray diffraction analysis, and the others used for elemental analysis.

Qualitative XRF scans were made of representative filter samples. These are shown in Figures 6-11. The filter blank spectra (Figure 6) shows high blank levels for a number of elements, high copper peaks are due to copper in the filter holder (Cu, Zn, Ni, Fe, Mn). Close examination reveals, however, that the following elements are observed:

Stainless Steel:	Fe, Cr, Mn, Ni
Mild Steel:	Fe, Mn
Brazing:	Cd, Zn, Ag, Cu, Sn

Thus, the qualitative analysis may be limited to a small number of elements. In the case of mild steel brazings, the brazing compound (Figure 12) contains a predominance of silver (Table 3), while in the fume, the silver is quite reduced when compared to cadmium (Figure 13). This interesting result is evidently due to the large difference in the boiling points of silver (2212°C) and cadmium (765°C).

3.2 Instrumental Parameters

The Philips AXS instrument permits different settings for instrument parameters such as goniometer 2θ, analyzing crystal, etc. Instrument parameter settings which maximized the recorded x-ray fluorescence intensity for each element of interest were determined using the fume samples

previously described, or facsimilies. The instrumental parameter settings were used in the remainder of this study are given in Table 5. In general, element peaks did not overlap and the parameter settings were easily determined. In two cases, however, overlaps did occur as discussed below:

MANGANESE: X-ray analysis of the first row transition elements is complicated by the close proximity of many absorption and emission lines. The effect of chromium on manganese is significant. In Figure 15 it is seen that the chromium Ka emission, 69.36°2â may add some intensity to that measured at the manganese Kb line position (62.97o2θ). Correction for this effect required substraction of the chromium contribution at this angle. This contribution is computed as some fraction of the chromium Ka intensity from a pure chromium sample, Figure 14. The computed intensity is 0.0158 x CrKa emission intensity. This small but necessary correction was applied to all manganese intensities if chromium Ka intensity was observed.

SILVER: As previously noted, silver exists in small amounts compared to cadmium in the brazing fume samples (Figure 12, 13).

Subtraction of the cadmium contribution to the intensity measured at silver Ka angle was not possible due to the large intensity differences between silver and cadmium. In this case, the silver La line was used. Although weaker than the Ka line, sufficient intensity from the La line could be obtained for successful analysis.

3.3 Deposition-Intensity Relationships

Fume samples were analyzed by XRF using the optimized instrument settings. Two analytical techniques were also used: atomic absorption spectroscopy (method of reference 10) and inductively-coupled plasma emission spectroscopy (Table 6). The ICP technique in our laboratories is in the developmental stage and should not be considered a primary standard. In particular, interelement effects known to exist in ICP were not corrected for because the correction factors had not been evaluated at the time of these investigations.

In Table 6, typical results for five fume samples at each of four loading levels (VL, L, M, H) are given for four elements (Fe, Ni, Cr, Mn) in plasma arc cutting fumes by the analytical methods AA and ICP along with the relative standard deviation. In addition, the students T-test of differences is given to indicate the degree of non-agreement between the AA and ICP results (if T is greater than 2.776, a significant difference exists at the 95% confidence level). The per cent difference (%) between the AA

and ICP result is also presented. The average XRF intensity (counts per second) is given, and the correlation between the AA and XRF results (perfectly linear = 1.00). It is evident that the AA and ICP results agree closely (vida infra), and that there is an excellent linearity between the deposition (by AA) and the XRF intensity, since most correlations are greater than 0.99. (This is demonstrated graphically in Figure 16 for plasma Arc cutting and in Figure 17 for the four metals in various welding fumes). Thus, we may conclude that the interelement effects in XRF are indeed minimal, and that a linear calibration curve can be utilized in subsequent analyses. This is exemplified by the case of manganese, for which an interelement effect is known to exist with chromium. That this effect is sufficiently corrected by the aforementioned algorithm is substantiated by the similarity of the concentration vs. intensity data slopes of manganese in mild steel (no chromium) and in stainless steel (containing chromium), Figure 17.

The variation in slopes within a single element for the different processes is primarily due to the changes in the XRF instrument over the time span (3-4 months) of the data gathering and analysis (except for stainless steel-MIG, see 3.3.2). This indicates the necessity for restandardization of the instrument for each analytical sequence.

3.3.1 AA vs. ICP Results

Useful to this study is a comparison of the analysis of the fume samples by atomic absorption and by inductively-coupled plasma atomic emission (ICP). The data of Table 6 indicate that, in general, the results are in good agreement for the elements under consideration. The average percent different for all determinations of fumes from stainless steel, stick fumes was 95.66 . However, the small differences that do exist are significant (at the 95 confidence level), as defined by the t-test of difference (AA vs. ICP) in Table 5 (i.e., most t-values exceeded 2.776). Apparently, a small, undetermined, consistent source of error is highly probable. As mentioned, the ICP was not fully operational at the time of these analyses. Consequently, no interelement corrections could be applied to the ICP results; this is a likely source of small consistent errors. The ICP has subsequently been updated to include these corrections for routine analyses.

3.3.2 Deposition Limits

The estimation of deposition (loading) limits is important for both the sampling protocol, and the XRF analysis. Assuming oxide forms for the elemnts, the most hghly deposited samples had the following dotal deposition weights: ~0.40 mg (stainless steel, stick), ~0.44 mg (mild steel, stick) and ~0.74 mg (brazing). The filters were visually quite colored. As heavier loadings are likely to create shadowing effects in the XRF analysis, and increase the opportunity for fume to fall off the filter, these approximate loading levels are probably near the maximum for the technique. At these loading levels, no loss of linearity of XRF intensity vs. deposition exists. However, if the deposits are disturbed, as was observed in the case of stainless steel MIG samples, then the data will be scattered and a lower calibration slope for all four elements may result. The stainless steel MIG samples were handled considerably more than the others (see Figure 17).

Different threshold limit values (TLV) exist for the various constitutents of welding fumes. The TLV for total welding fume is 5 $mg/_m{}^3$[21]. Therefore, a two-hour sampling at 1.0 LPM at a fume concentration corresponding to the TLV level of total welding fume would collect 0.6 mg of fume. This would correspond roughly to the loadings described above.

In conclusion, it is recommended that loadings be less than 1 mg, which can be judged visually as a highly colored but even deposition, be the limit for routine sampling.

3.3.3 Concentration Intensity Relationships

Are important conclusion of the previous work is the choice of a suitable algorithm for relating measure XRF intensity (I_i) with the weight (C_i) of an element I on a filter sample. It is observed that a sample straight line relationship will suffice:

1. Straight-Line, (SL) $C_i = A_iI_i + K_iB_i$

   Where B_i is the Background intensity, and A_i and K_i arc constants to be determined for a particular system.

The Philips AXS system is capable of more sophisticated relationships which we discuss for the sake of completeness. They are:

2. Lucas - Tooth/Pyne, (LP)

$$C_i = (A_iI_i + K_iB_i)\ (1+ \sum_j A_{ij}I_j)$$

3. Lachance/Traill, (LT)

$$C_i = (A_iI_i + K_iB_i)\ (1+\sum_j A_{ij}C_j\ )$$

4. Rasberry/Heinrich, (RH)

$$C_i = (A_iI_i + K_iB_i)\ [\ 1+ \sum_j a_{ij}C_j + \sum_k \left(\frac{C_k}{1 + C_i/100)}\right)]$$

Where A_i, I_i, K_i, B_i are as above, I_j, C_j, and C_k are the analogous quantities relating to interfering elements (j) in the sample, and A_{ij}, a_{ij} and B_{ij} are constants to be determined iteratively. These latter three relationships allow for the correction of interelement effects explicity. Thus, they appear to have considerable advantage over the SL relationship. These relationships, however, have been developed for use in traditional XRF analysis: the determination of small per cent concentrations of an element in a matrix. In welding fumes, however, the relative composition of the contributing elements does not vary, only the amount. Consequently, relationships based on Cj are not usable, viz., the LT and RH equations [20].

Of the remaining two relationships (SL and LP), our investigation of deposition-intensity data adequately verifies the utility of the SL relationship.

A thorough investigation of the usefulness of the LP Relationship for the reduction of welding fume data has been performed. Because of the regularity in the composition of the standards used, it is impossible mathematically to determine the LP constants required to allow calculation of fume depositions to a degree superior to that accomplished by the SL relationship.

3.4 Summary

It is seen that simple, linear calibration curves for the reduction of fume analysis data is quite possible. No non-linearity is noted, and the intercept is generally near zero. As abscence of interelement effects is apparent.

Two significant drawbacks do exist. First, standardization by this scheme requires that four to six equivalent welding fume samples of at least three different deposition levels must be obtained. Half the samples at each deposition level must be ashed and analyzed by atomic absorption.

Secondly, elements that are in low concentration in the standard filters will not be analyzed accurately by AA or XRF. These elements, consequently, will not be represented by as good a calibration curve as more heavily depositioned elements.

4. Analysis of Field Samples

Field samples of welding and brazing fumes were obtained during February, 1980 at three area welding establishments. They will be designated locations I, II and III, described as follows:

I Welding school, mostly mild steel welding occurring, February 5.

II Manufacturing plant, brazing and stainless steel-stick welding, February 15.

III Manufacturing plant, stainless steel and carbon steel, MIG, stick, and automated welding, February 21.

In all three locations, both personal and area sampling were taken. Dupont personal sampler pumps with preset timing were used for personal smapling; a six-position, limiting-flow orifaced cassette assembly built at NIOSH was utilized for the area sampling. Mr. Jim Bioano, an industrial hygienist from DSHEFS, NIOSH, assisted the author in all three locations.

4.1 Qualitative Analysis

The fume sample analysis began with a qualitative scan of representative samples to fix the elements to be determined quantitatively. These scans are presented in Figures 18-20 (Figure 18, upper, is a scan of the filter blank). The copper lines at each 45.08 and 40.56 2θ are artifacts due to the instrument and sample holder. Examination of the sample scans reveals that quantitative analysis is required on the elements Ti, Cr, Mn, Fe, Co, Ni and Zn. Background corrections are not expected to be unusual. In addition, we see that these scans resemble those of welding fumes generated at NIOSH. Consequently, parameters from the NIOSH-produced welding fume

samples and related studies will be sufficient for the quantitative analysis of the field samples for all elements.

4.2 Instrument Characteristics

4.2.1 Standard Curves

Standardization curves for quantitative analysis were produced as follows. Welding samples on stainless steel (310 steel with 310-14 rods), six each at low, medium low, medium high, and high levels, were obtained with the NIOSH welding station fume sampler described previously. A similar set of samples was obtained from brazing on mild steel (with Sta-flo 45). Three samples of each level were analyzed for element deposition by AA (reference 16) and ICP, and three were analyzed by XRF. The result was deposition vs. XRF intensity data in triplicat at four levels for each of the six elements of greatest interest. (Eleven elements are available with ICP). This data is presented in Table 8 and is graphically displayed in Figure 21 (the ICP data is described by the dashed lines in Figure 21, and by all of Figure 22; dotted linies denote the standard deviation limits of the data.

4.2.2 Minimum Detection Limits (MDL)

The background (noise) intensities with Millipore AAWP filters for the elemetns of interest are quite low. Conseqneutly, the minimum detection limits for the elements of interest are quite low. The MDL values were computed according to the formula

$$MDL = \frac{3}{m}\sqrt{\frac{I_b}{T_b}}$$

Where m is the slope of the calibration curve, I_b and I_t are the measurement durations (100 seconds) and background intensities for the particular analyte element. The MDL's by ICP or AA do not differ significantly; they are listed below as computed from the more extensive ICP data:

Analyte	MDL (ug/filter)
Ti	0.01
Cr	0.10
Mn	0.11
Fe	0.08
Co	0.12
Ni	0.08
Zn	0.14
Ag	0.01
Cd	1.29

4.3 Quantitative Analysis

4.3.1 Deposition - Intensity Plots

XRF analysis of the field samples and the calibration standards were completed within a three-day period to evade instrument instability. For each element, the XRF intensity of the calibration standard at a particular loading level was matched with the average deposition of the twin standard filter which had been ashed and analyzed by AA (or ICP). Two sets of calibration urves were thus generated, one based on AA analysis and one based on ICP analysis of the standard filters. The XRF intensities of the field samples were then converted to metal depositions twice, once with the AA and once with the ICP based calibration curves (Figure 21 and 22). We first examine the data via deposition-intensity plots (Figures 23 and 24). We would like the calibration curves to follow the field sample data closely, indicating goodness of the calibration curves. In general, they do; however, in other cases, puzzling differences exist which are partly due to the sample loadings. For example, the consistently low calibration curve for nickel (Figure 23, upper left) appears quite close to that field sample data when the coordinates of the plot resemble those expected for a heavier deposition (Figure 23, right middle). For zinc, it is seen (Figure 23, bottom left) that most field samples have only background (2ug) amounts of zinc with a few (from Location II) with high depositions. The elements Co, Ag, and Sn are not deposited significantly.

4.3.2 Numerical Results

As mentioned above, two sets of analytical results were derived from the XRF intensities, one from the AA calibration, and one from the ICP calibration data. The field samples were then ashed and analyzed by AA and ICP. The XRD results were compared, respectively with the results of the analyses by AA and by ICP. The AA-based data set, expressed in $mg/_m3$ (air concentrations) for each field sample, is given in Tables 9, 10 and 11 for field locations I, II and III, respectively, and summarized in Table 12. Raw data for both AA and ICP based data sets, in ug/filter, is summarized in Appendix 1 and 2.

In Table 12, the difference D (AA OR ICP value - XRF value) and the Bias (D/AA [OR ICP] value X100) indicate that the XRF method is about as precise as the AA method where significant deposition exists. Large basis appear when the depositions (and consequently the D values) are low. The biases in Tables 12 sometimes, however, exceed the NIOSH requirement (17) of less than 10 percent, if we accept the AA results as "true". It should be kept in mind that the statistical protocol described in Reference 17 does not exactly apply here, however, as replicate samples at 1/2, 1, and 2X the OSHA or NIOSH standard are not analyzed. In the data reported here, many near-zero depositions greatly detract from the usefulness of bias and t-statistic data. More significant is that, in general, the difference in mg/m^3 comparing XRF and AA (or ICP) is small. The student's t-test of

differences, when t is greater than t of 95% significance, indicates that a small but significant error persists between the XRF and the alternate method, whether the latter is AA or ICP. The cause of this difference is not obvious, with no relationship apparent in the differences in AA, ICP, and XRF results. It is likely that the standardization method utilized should be investigated for possible improvements. Initial consideration of alternative standardization techniques has begun (See section 4.4); this is an area of study included in upcoming project plans at NIOSH.

4.3.3 Individual Elements

The analytical results for the various elements are not all identical and, consequently, are discussed individually below (based on data in Appendix 1 , Tables 1 and 2).

TITANIUM: Titanium was calibrated by ICP only (Figure 24). XRF results calculated from the ICP calibration data in Table 8 were compared to the ICP analysis of these samples. They differ by an average of 28.4%. However, the titanium depositions were quite low (less than 2.5 ugm). The average difference between the XRF and ICP results was only 0.3 ug filter.

CHROMIUM: Chromium was found at depositions of 6 ug. At this level, the element was easily detected by either AA- or ICP-based standards with an average difference (AA-XRF), of 0.07 ug (or 0.3 ug with ICP). The percent error of -2.44% (AA vs. XRF) is excellent but probably fortuitous considering the low deposits of many samples; the corresponding percent for ICP is -13.13%.

MANGANESE: Manganese was found in amounts of 0-10 ug. The standard curves appear low (Figure 23, 24). This may be due to a residual matrix effect since chromium and iron are known to absorb the particular wavelength of X-rays which excite Mn Ka radiation. The average difference, AA-XRF is 1.5 ug (AA); AA-IPC is and 0.8 ug for the three locations. The bias is 43.48% (AA) and 14.19% (ICP).

IRON: Iron was the most common heavily deposited element, 0-20 ug. However, only six samples (from location I) had more than 5 ug of iron. These were diluted twice for the AA analysis which may account for the high errors in the AA vs. XRF data for these six samples (bias of 32.6%, 34.6 ug average difference; the corresponding numbers of the ICP-based data are 13.4% and 13.7 ug). For the entire set of field samples, the biases are 11.84% , 6.2 ug (AA) and 0.7%, 1.6 ug (ICP).

NICKEL: This element was found in low amounts only (less than 1.5 ug). Field samples from location I only were analyzed by AA; the average difference between AA and XRF results was only 0.4 ug. All three locations were analyzed by ICP; the ICP minus XRF difference is 0.2 ug.

ZINC: Zinc was found in high quantities (30-70 ug) only in E1-6 of location II near a galvanized metal welding operation. Here, AA-XRF depositions differed by an average of -2.22 ug or -10.86% (-5.26 ug or -10.01% for ICP). Other depositions were very low, i.e., near blank value levels (about 1 ug).

OTHER ELEMENTS: Silver, tin, and cobalt calibration curves were obtained using ICP standardization and were used to convert the XRF intensities of the field samples to concentration values. However, only random background depositions were computed. No good correlations between the XRF intensities and the ICP-determined concentration levels were obtained.

4.3.3 Absorption Corrections

A generally accepted correction for X-ray fluorescence analysis is the effect of the absorption of x-rays by the sample matrix (Reference 15. 119). Both absorption of the primary (exciting) x-ray beam, and absorption of the emitted characteristic line must be corrected. The effect of absorption is as follows:

$$I = I_o e^{-u/t} = I_o e^{-du/p} \quad \text{if } t = p/d$$

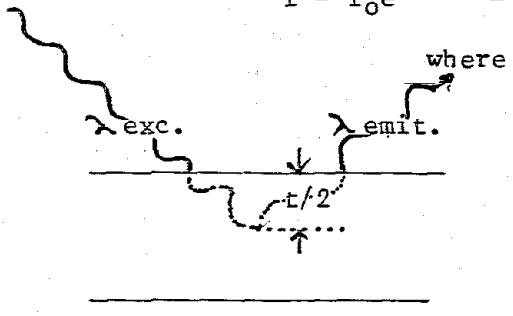

I	=	Resulting x-ray intensity
I	=	original x-ray intensity
u	=	absorption coefficient
t	=	sample thickness
u/p	=	mass absorption coefficient, cm^2/gm
d	=	deposition density, $gms/_{cm^2}$.

Tables of u/p are available (Reference 15, p. 972). The deposition density, d, can be estimated from the results of a preliminary analysis. Assuming the exciting radiation passes through half the thickness of deposit before exciting an atom to emit, the photon trace thus passes through half the total deposition twice, at approximately 45°C to the plane of the deposition. Consequently, the total absorption coefficient for each absorbing element is:

$$\frac{ud}{p} = \sqrt{2}\left(\frac{u}{p}\ \frac{d}{2}\right)_{excit} + \sqrt{2}\left(\frac{u}{p}\ \frac{d}{2}\right)_{emit}$$

Consider the field sample B10. Assume excitation by chromium Ka, (λ = 2.291 A). From the ICP analysis, we can determine the elemental depositions, using the area of deposition of 9.621 cm^2. We construct the following table using data from reference 15, page 972:

Element	Deposition, ugm	u/p, Excitation	u/p, Emission	utx10^6
Ti	0.7	537.8	378.6	47.1
Cr	3.0	246.4	480.1	160.2
Mn	3.1	106.5	63.0	38.6
Fe	44.4	119.2	70.6	619.1
Co	2.6	133.0	78.8	40.5
Ni	1.1	147.5	91.2	19.3
Zn	1.2	163.5	111.6	24.3
Ag	0.3	690.6	426.7	24.6
Cd	0.2	735.8	454.9	17.5
Sn	2.0	874.9	540.6	208.1

Total $1199.3X10^{-6}$

Then, $I = I_o e^{-ut} = I_o\ (0.9988)$, or an error of about 0.12%. Thus, absorption corrections can be assumed to be negligibly small for these very thin depositions.

4.4 Other Standardization Techniques

The present method of calibration, using matched sets of generation system welding samples, is not readily applicable to typical laboratories analyzing routine samples. Two other methods of calibration are described in the literature and were initiated in this study in order to provide direction for future research.

4.4.1 Multiple-Drop Method

A set of standard filters (Type A2) was purchased from Columbia Scientific Company, Houston, Texas. These filters were deposited by the multiple-drop technique with Ti, Cr, Fe, Ni, Zn, and Cd at three concentrations: 1, 5, and 10 $ug/_{cm}2$. These filters were analyzed by XRF to construct calibration curves, which were compared with the deposition vs. XRF intensity (ICP calibration) for the field samples (Figure 25). The large deviation of the calibration curve prepared with the type A2 commercial standards (dashed line, Figure 25) indicates that use of those commercial standards will not result in data comparable to ICP results, especially for Cd. On the basis of these data, we cannot recommend these commercial standards for the calibration of the XRF instrument.

4.4.2 Filter Deposition Method

A second method of standardization employs the deposition of metal particulates from isopropanol dispersions of sieved multielement powder standard (Spex Mix 1000) onto Gelman DM450 filters. This method follows closely that of Semmler, et. al[19]. Five, ten, and fifteen mL of approximately ug/mL 200 ppm isopropanol solution of the above standard, drawn through the filter in buchner funnel apparatus with a light vacuum, with resulted in an even, reproducible deposition of the solid on the filter. After XRF analysis, the filters were ashed by oxygen RF plasma and analyzed by AA. A comparison of the resulting intensity vs. deposition data (Figure 26a) reveals the good linearity of the curve. It is closely mimics the response of the field samples for Fe, Ni, and Mn (Figure 26b). A similar experimental sequence utilizing ICP analysis gave similar results, Figure 26c. The results for chromium were not acceptable. This experiment indicates the promise of this method of calibration, which will be pursued in future experiments.

4.5 Instrument Difficulties

Although the Philips AXS x-ray fluorescence system works well when it is operating, a large amount of down-time due to a variety of failures has delayed the work. No real improvements in the per cent reliability have been noted to date. Consequently, the author is reluctant to recommended this model of XRF instrumentation to prospective buyers.

5. Conclusions

This study was initiated to investigate the feasilibity of the X-ray fluorescence technique for the analysis of welding and brazing fumes. This required:

1. Building an adequate fume generation device;
2. Elucidation of the physical characteristics of typical welding and brazing fumes;
3. Determination of the extent of elemental interferences;
4. Establishment of a suitable set of standards; and
5. Complete analysis of field samples by XRF and by an independent method.

Each of these subgoals has been successfully completed. The field sample analysis indicates the method has reasonable accuracy and precision compared to AA or ICP, with the single greatest detrimental factor perceived as inadequate standardization. Preliminary work with the solid dispersion deposition method for calibration indicates that this problem is tractible via an economical, rapid standardization procedure. More work is planned on the calibration problem so that a method can be written for routine analyses.

6. Acknowledgements

The following individuals contributed significantly to the work described in this report:

Mr. R. DeLon Hull and Mr. Mark Millson performed all the ICP analyses reported. Dr. Donald D. Dollberg and Mr. Martin Abell provided technological support in questions concerning the techniques of X-ray analysis. Mr. Rick Hornung provided advice on the statistical procedures used. Dr. David Taylor provided significant encouragement and guidance in the general direction of the project. Mr. John Crable, Dr. Dollberg, and Dr. Taylor formed a protocol review committee which set the protocol for this work. Ms. Anna Silvers and Ms. Teri McKee worked assiduously typing and correcting the manuscript and tables.

REFERENCES

1. "OSHA Takes Aim at Welding Fumes," Business Week, May 21, 1979, p. 126j. For complete biblography, see Reference 5.

2. "Welding Handbook", Volume 1, American Welding Society, 7th Edition, 1976, p. 34.

3. Ibid, p. 2.

4. "Welding" E. A. Fenton, Science and Technology, 22, p. 241

5. "The Welding Environment," American Welding Society, Miami, FA, 1973.

6. "Criteria for a Recommended Standard. . .Occupational Exposure to Welding and Brazing Fume." (Draft), DHEW, (NIOSH), 1979.

7. Dr. P. Baron, Private Communication

8. Electron Spectroscopy Photographs Courtesy of Dr. L. Stetzler

9. R. M. Stern, "A Chemical, Physical, and Biological Assay of Welding Fume. Part 1. Fume Characteristis," The Danish Welding Institute, 1977.

10. P. Grenfelt, A. Akerstrom, and C. Brosset, "Determination of Filter-Collected Airborne Matter By X-Ray Fluorescence," Atmos. Environ. 5, 1 (1971).

11. S. Kimura, M. Kobayashi, and S. Maki, "Some Considerations about Fumes Generated in Arc Welding Processos," IIW document VIII - 687-76.

12. K. Homma, H. Yamguchi, T. Yagami, H. Sano, and Y. Araki, "Industrial Health Aspects on the Arc Welding by Austenitic Filler Metals," IIW Document VIII-714-77.

13. R. F. Heile and D. C. Hill, Weld. Res. Supp., July, 1975, p. 201s

14. D. G. Howden, Weld. Res. Suppl., march, 1969, p. 125 s, and references therein.

15. E. P. Bertin, "Principles and Practice of X-Ray Spectrometric Analysis," 2nd Edition, Plenum, N.Y., 1978.

16. D. G. Taylor, Ph.D. "NIOSH Manual of Analytical Methods," DHEW (NIOSH), 2nd Edition, Vol. 5, 1979, P CAM. 173.

17. D. G. Taylor, R. E. Kupel, and J. M. Bryant, "Documentation of the NIOSH Validation Tests," DHEW (NIOSH), 1977, p. 3.

18. D. W. Schoeninger and C. A. Insko, "Introductory Statistics for the Behavioral Sciences," Allyn and Bacon, Boston, 1971, p. 173.

19. R. A. Semmler, R. D. Draft, and J. Puretz, in "X-Ray Fluorescence Analysis of Environmental Samples, T. Dzubay, Ed., Ann Arbor, 1977, p. 181.

20. John Croke, Philips Instruments, Personal Communication.

21. "Threshold Limit Values for Chemical Substances and Physical Agents in the Workroom Environment with Intended Changes for 1980," American Conference of Government Industrial Hygienists, Cincinnati, Ohio, 1980.

Figures

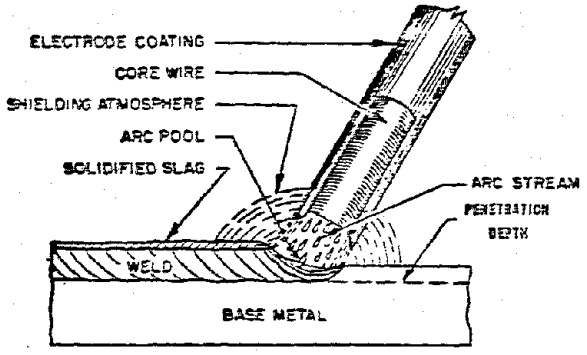

Diagrammatic sketch of shielded metal-arc welding.

SMAW

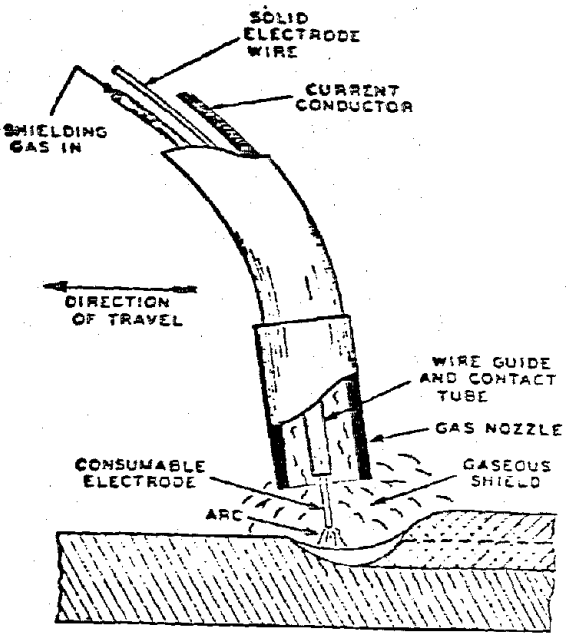

Diagrammatic sketch of gas metal-arc welding.

MIG

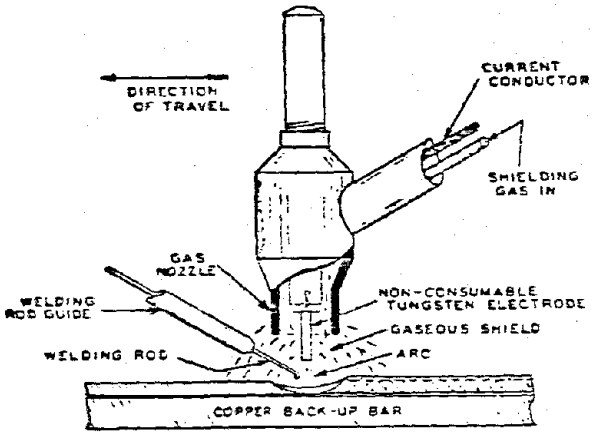

Diagrammatic sketch of gas tungsten-arc welding.

TIG

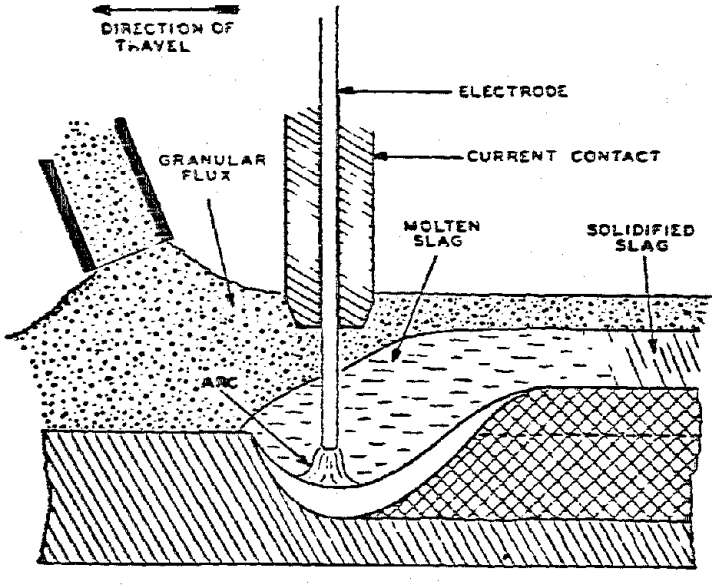

Diagrammatic sketch of submerged arc welding operation on heavy plate.

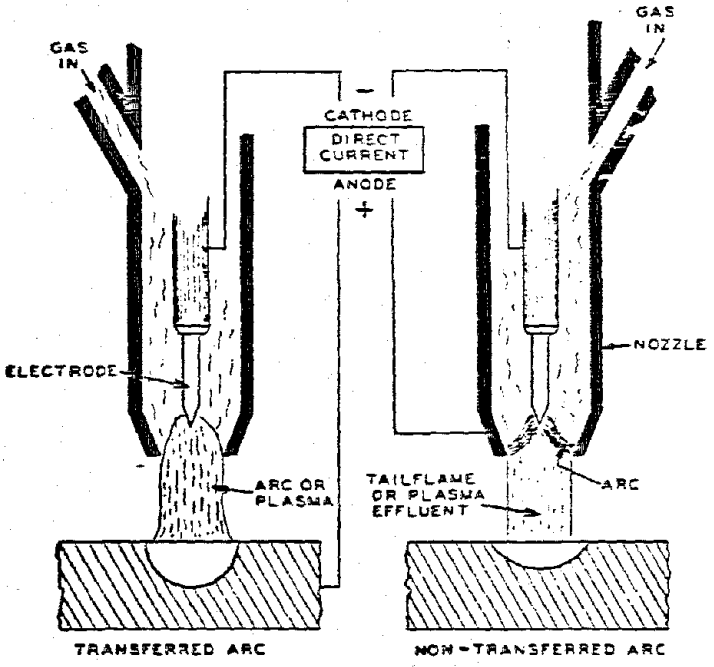

Diagrammatic sketch of plasma-arc process (transferred arc is used for welding).

PLASMA

FIGURE 1. Common Welding Processes
(From reference 5)

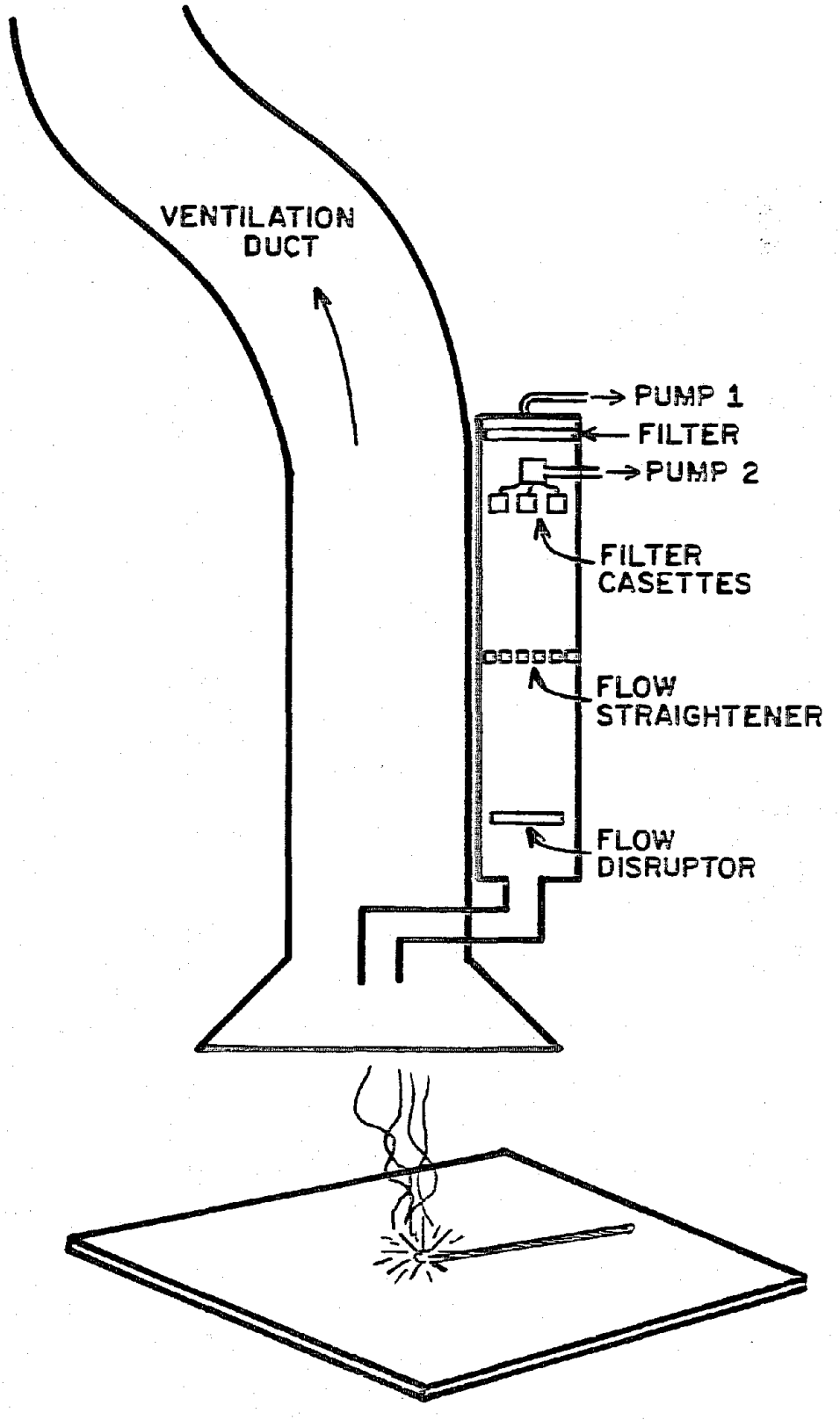

Figure 2

FUME COLLECTOR APPARATUS

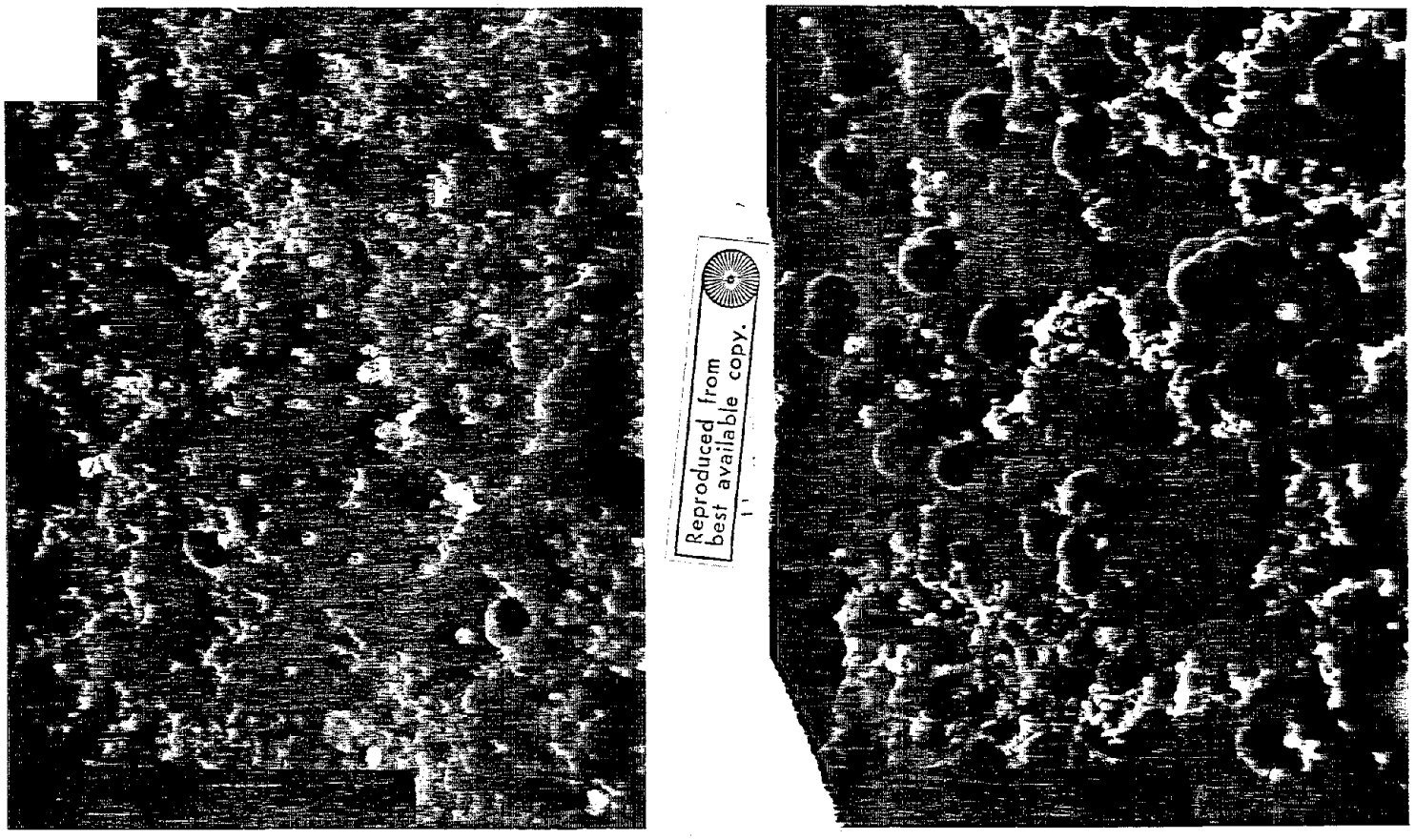

Figure 3A. Stainless steel, stick fumes, 6000x. Figure 3B. Mild steel, stick fumes, 6000x.

Figure 3C. Mild steel, stick fumes, AAWP, 6000x. Figure 3D. Stainless steel, stick fumes (6000x

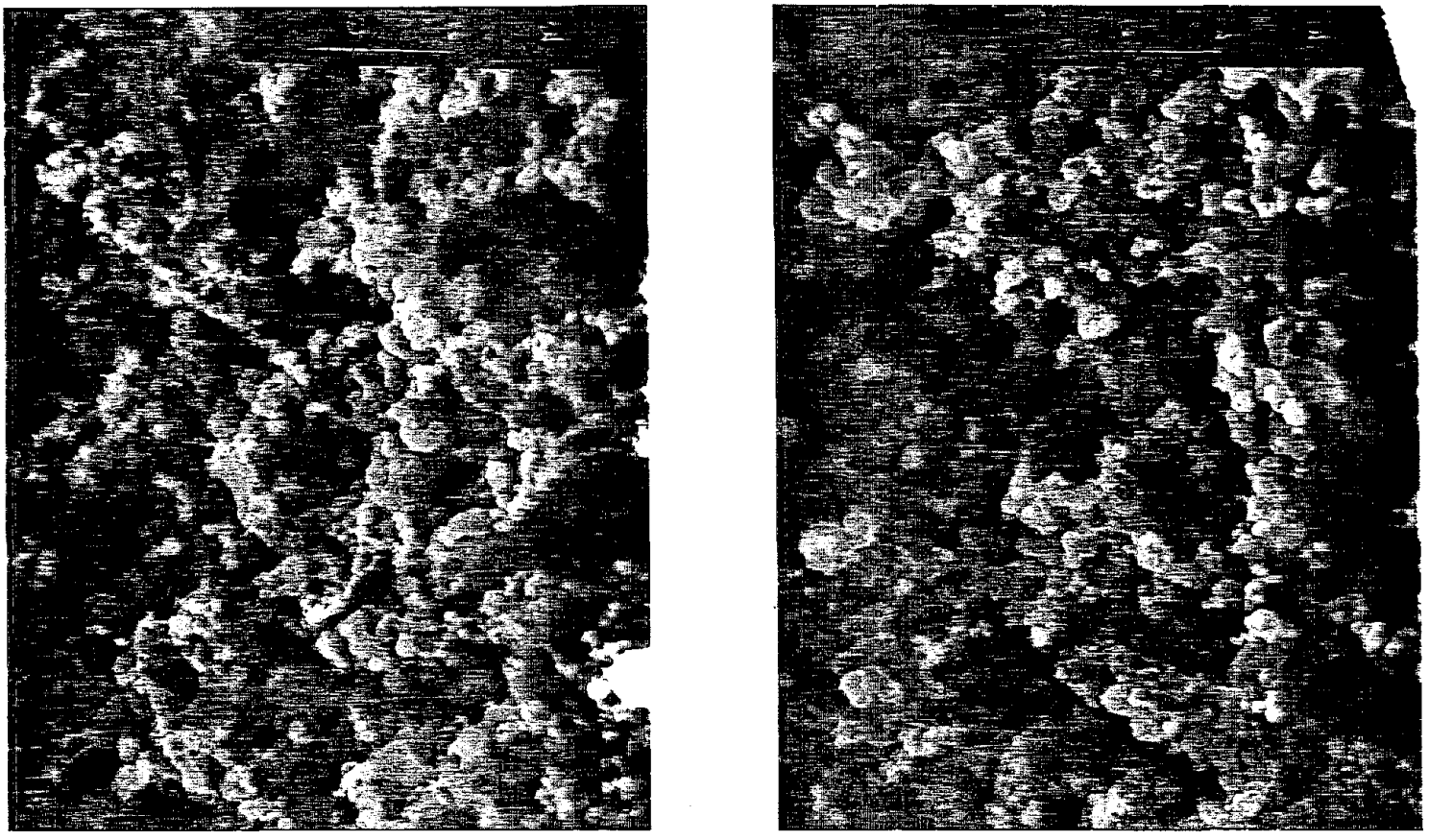

Figure 3. Photomicrographs of welding fumes on AAWP and Nuclepore filters.

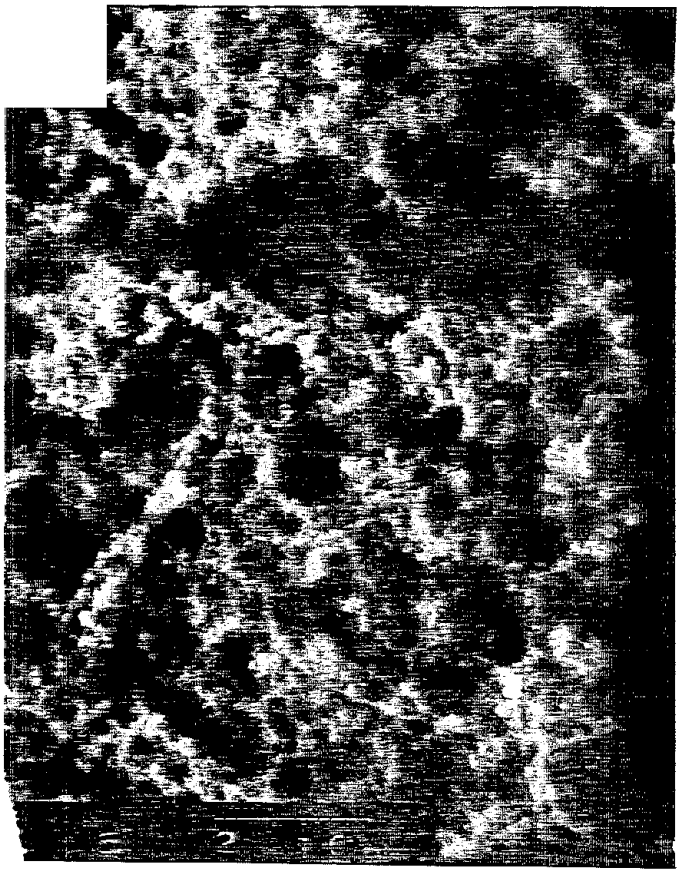

Figure 4A. Stainless steel, MIG fumes, AAWP, 6000x.

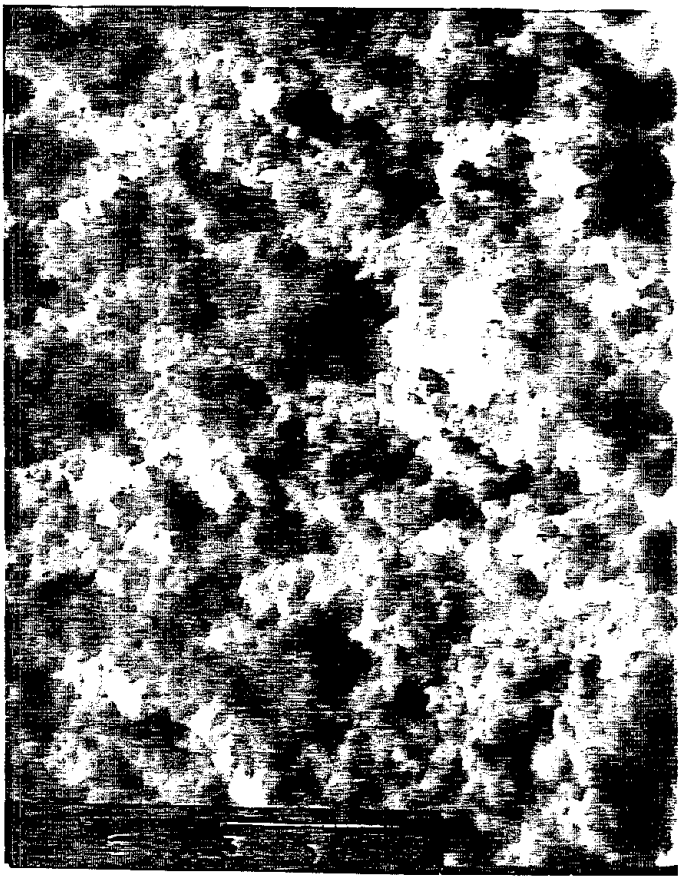

Figure 4B. Stainless steel, stick, AAWP, 6000

Figure 4C. M-1d steel, braze, AAWP, 6000x.

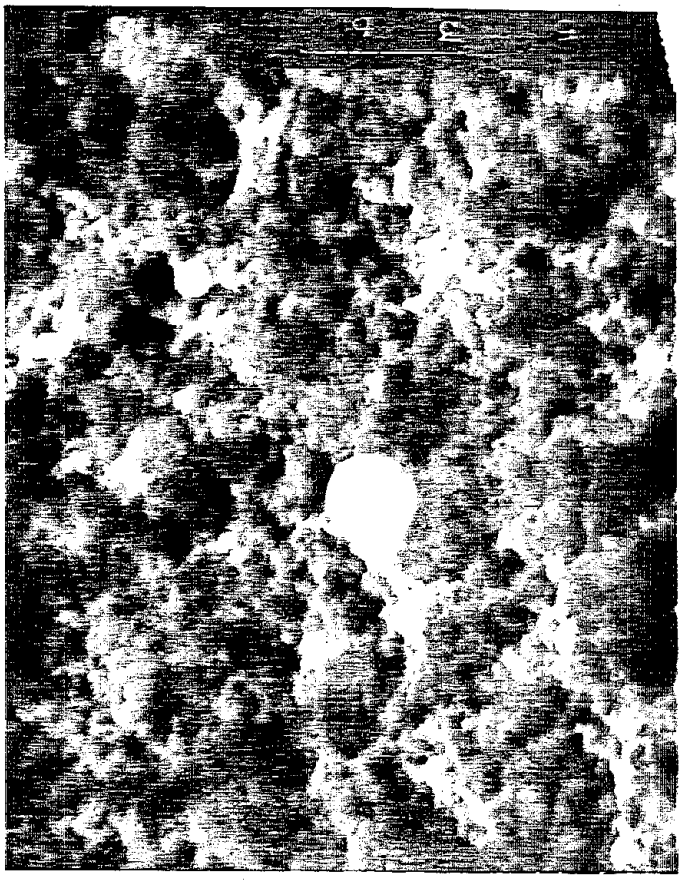

Figure 4D. Stainless steel, plasma arc, 6000x

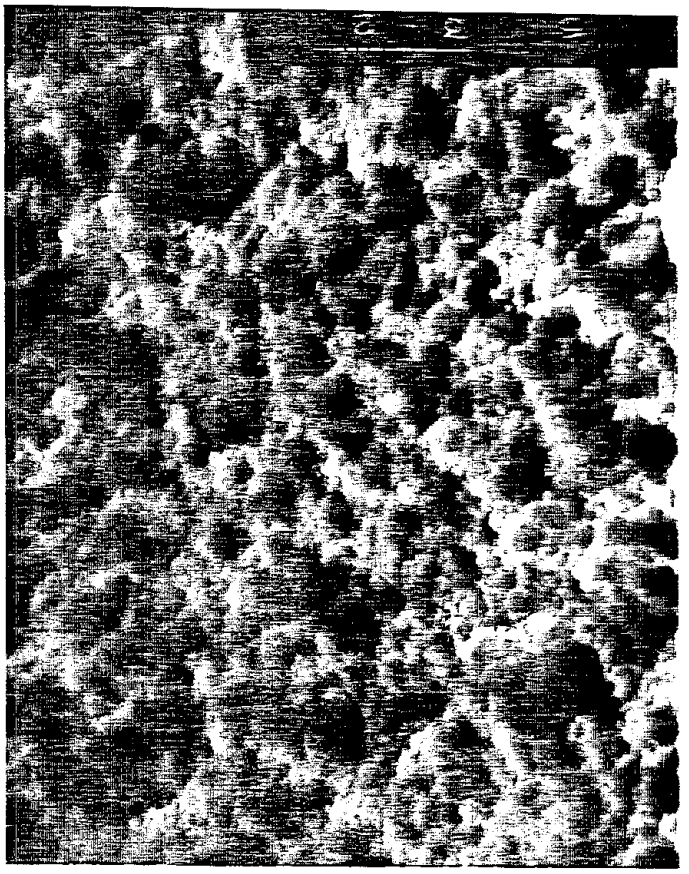

Figure 4. Welding fumes deposited in AAWP filters.

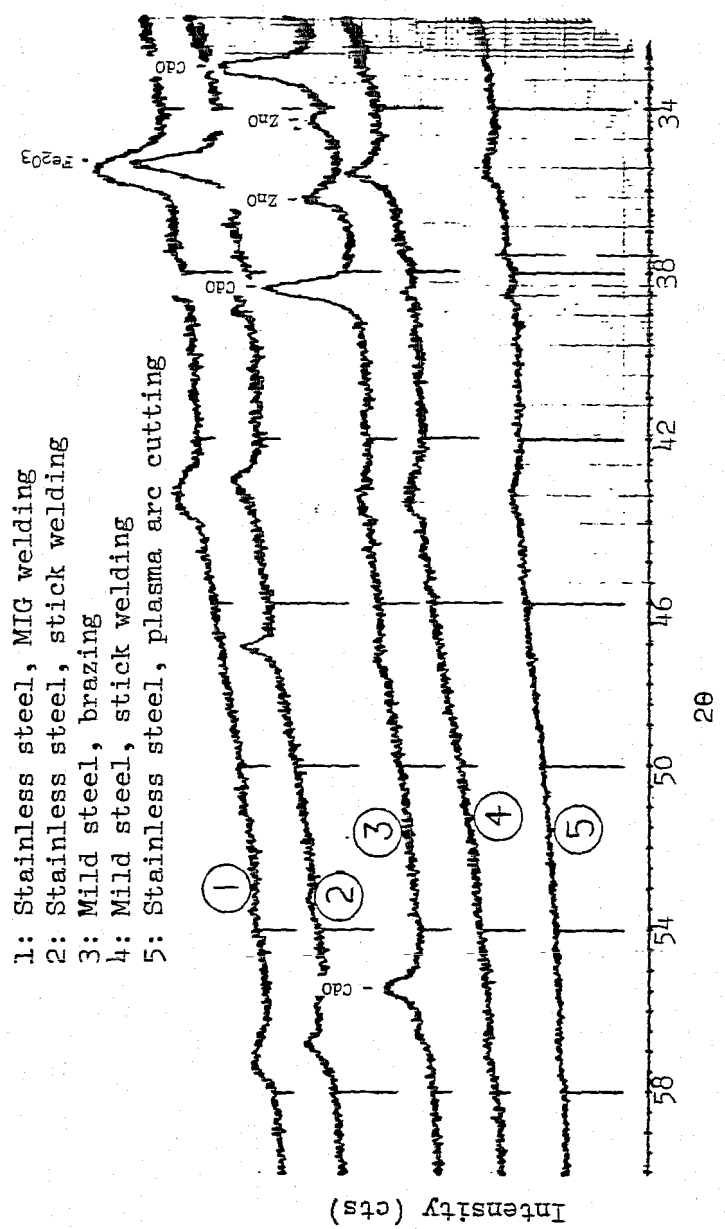

FIGURE 5

X-ray diffraction patterns of welding and brazing fumes.

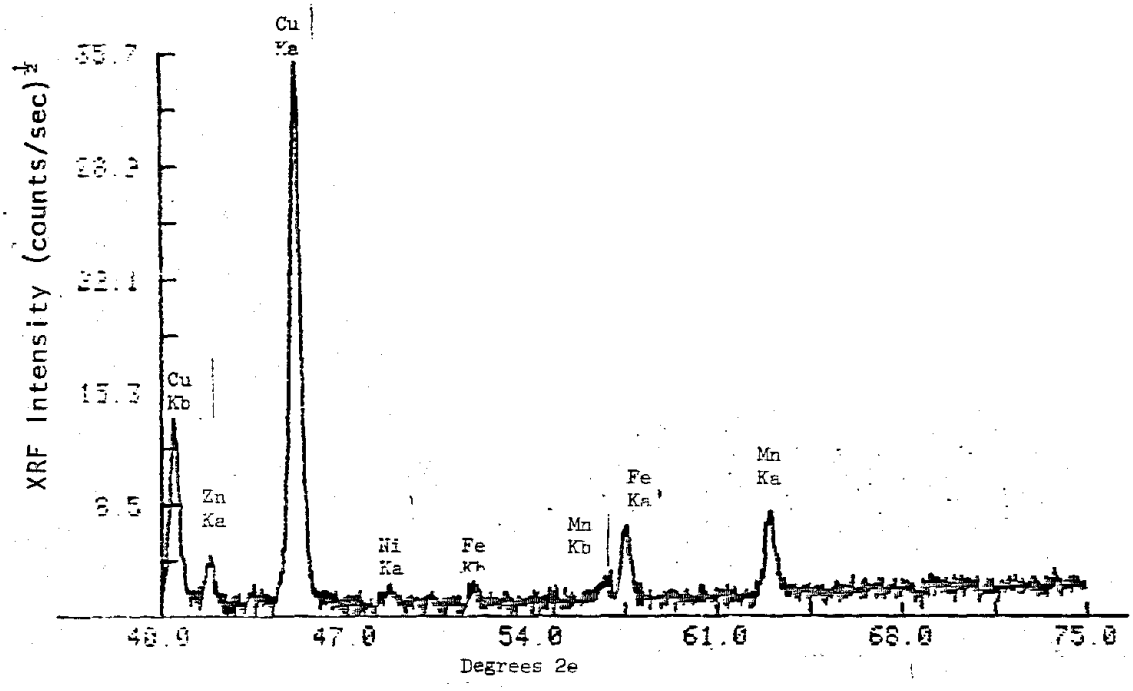

Figure 6. XRF 2e scan of AAWP filter blank.

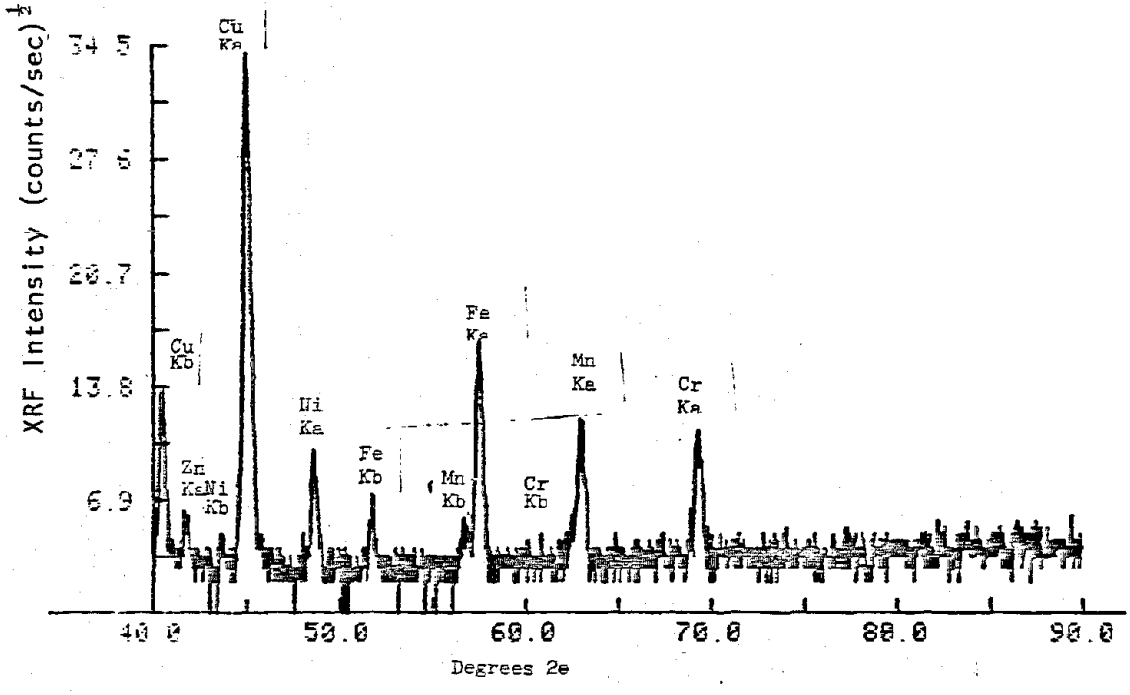

Figure 7. XRF 2e scan of stainless steel, stick welding fume on AAWP filter.

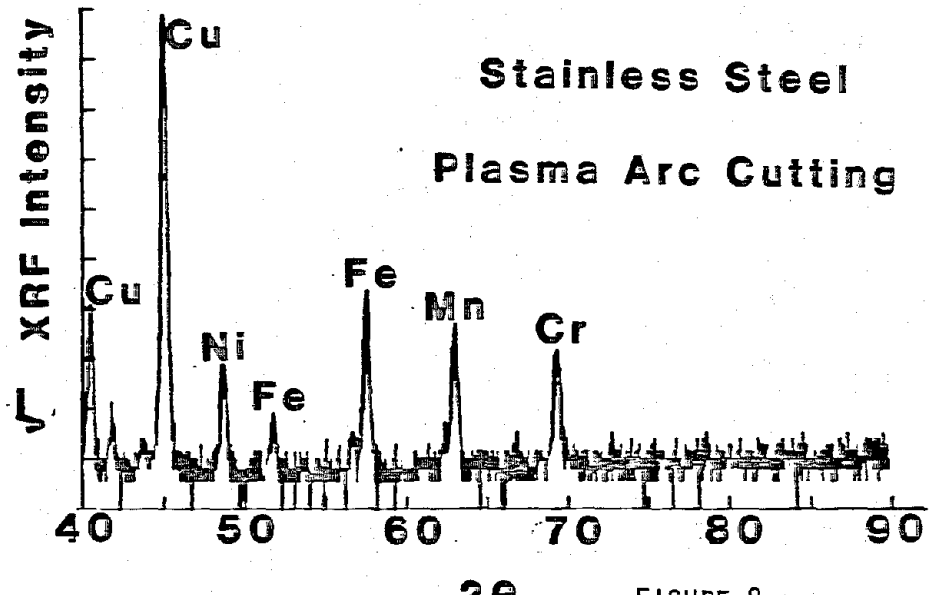

FIGURE 8
XRF 2θ scan of stainless steel, plasma arc cutting fume on AAWP filter.

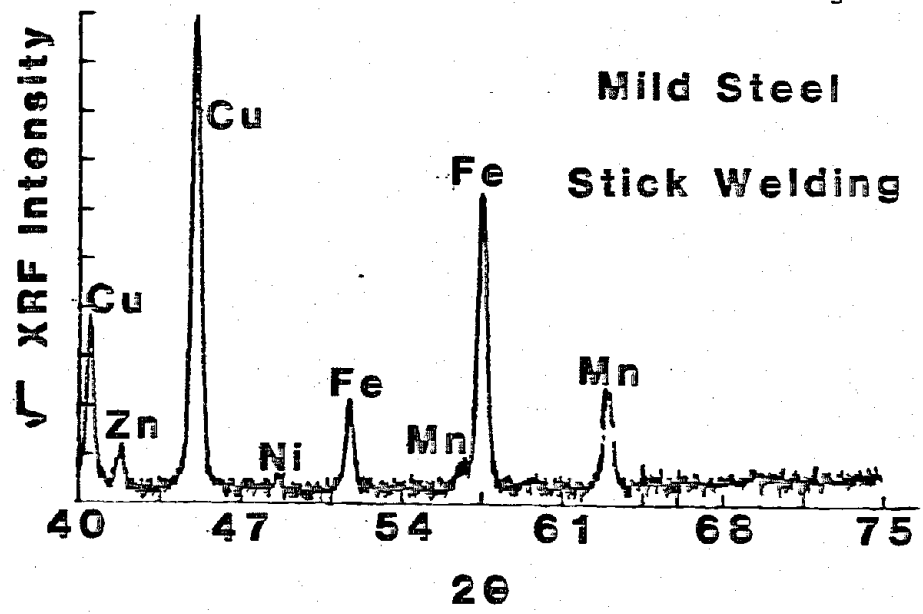

FIGURE 9
XRF 2θ scan of mild steel, stick welding fume on AAWP filter.

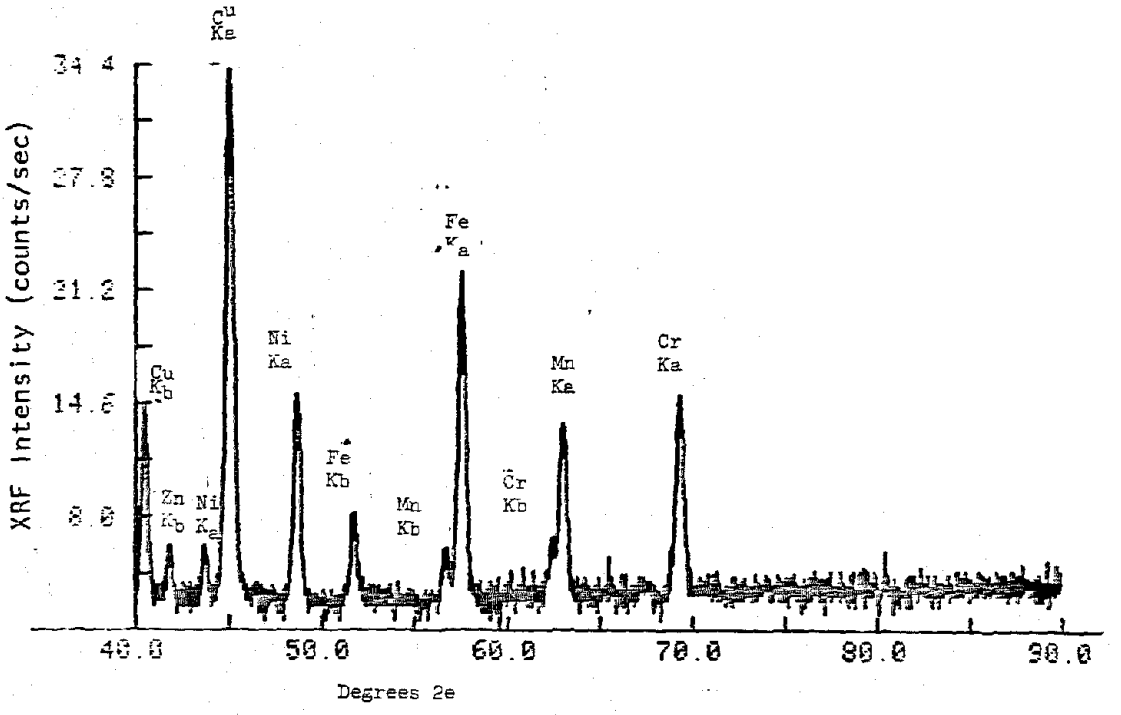

Figure 10. XRF 2e scan of stainless steel, MIG welding fume on AAWP filter.

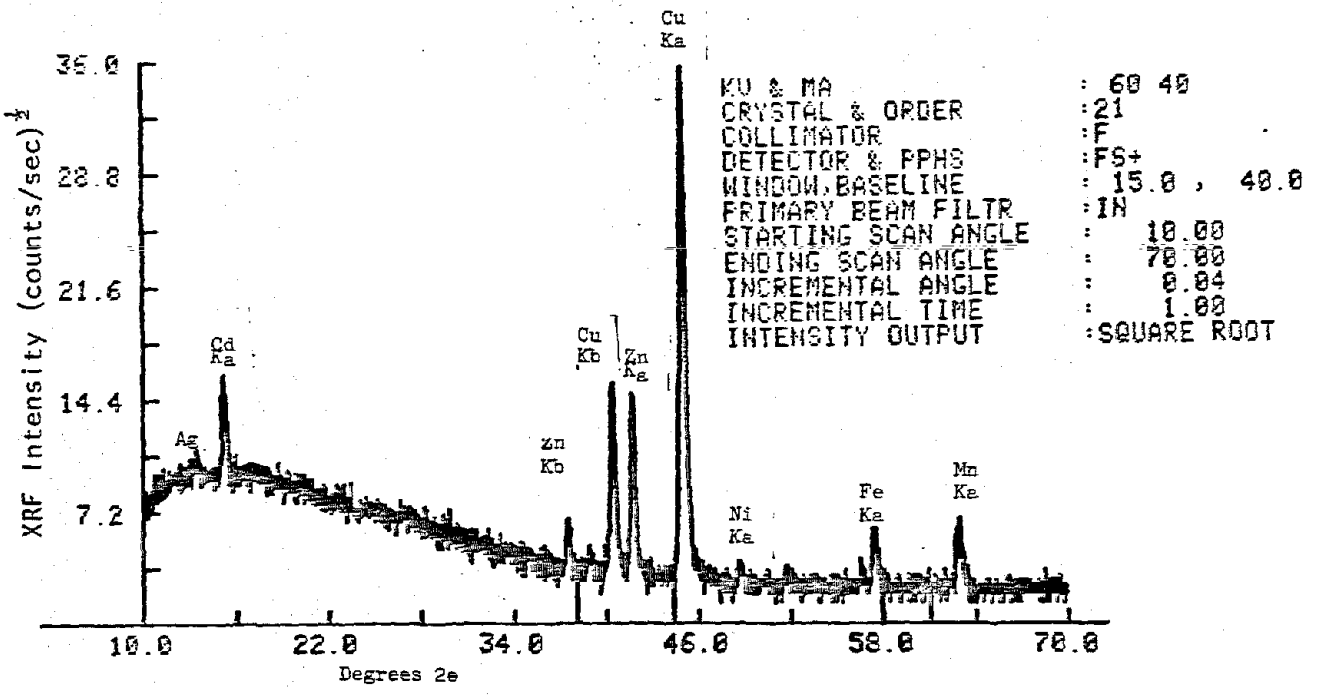

Figure 11. XRF 2e scan of StaFlo-45 brazing fume on AAWP filter.

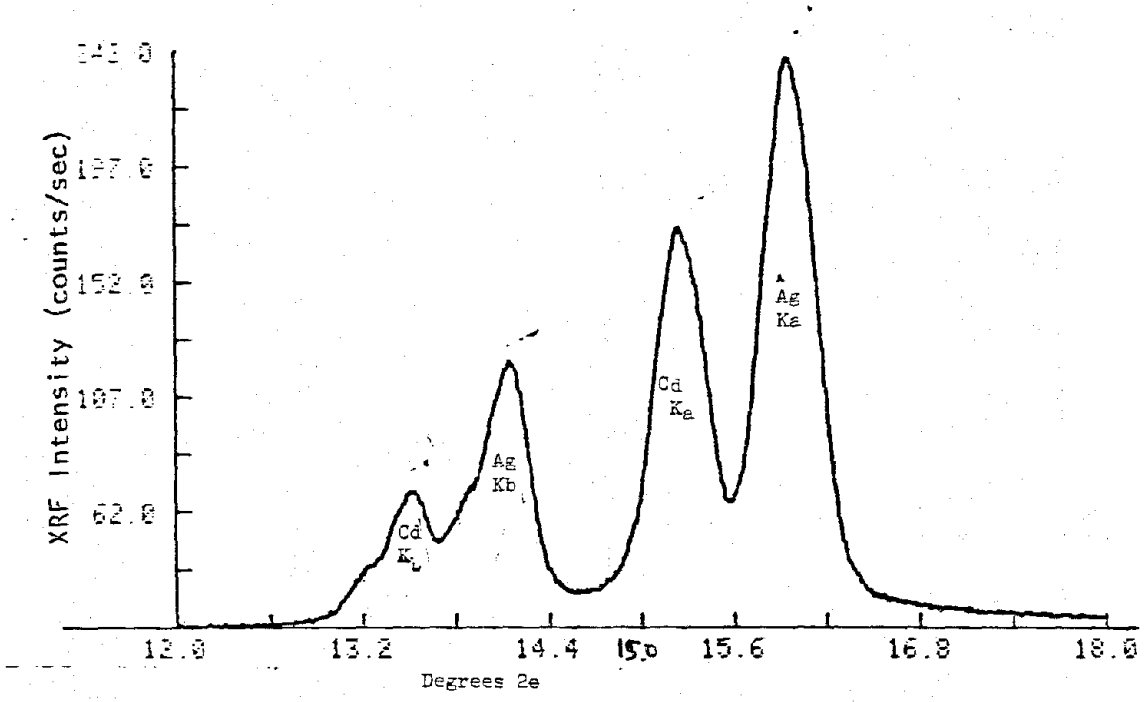

Figure 12. XRF 2e scan of STaFlo-45 brazing wire.

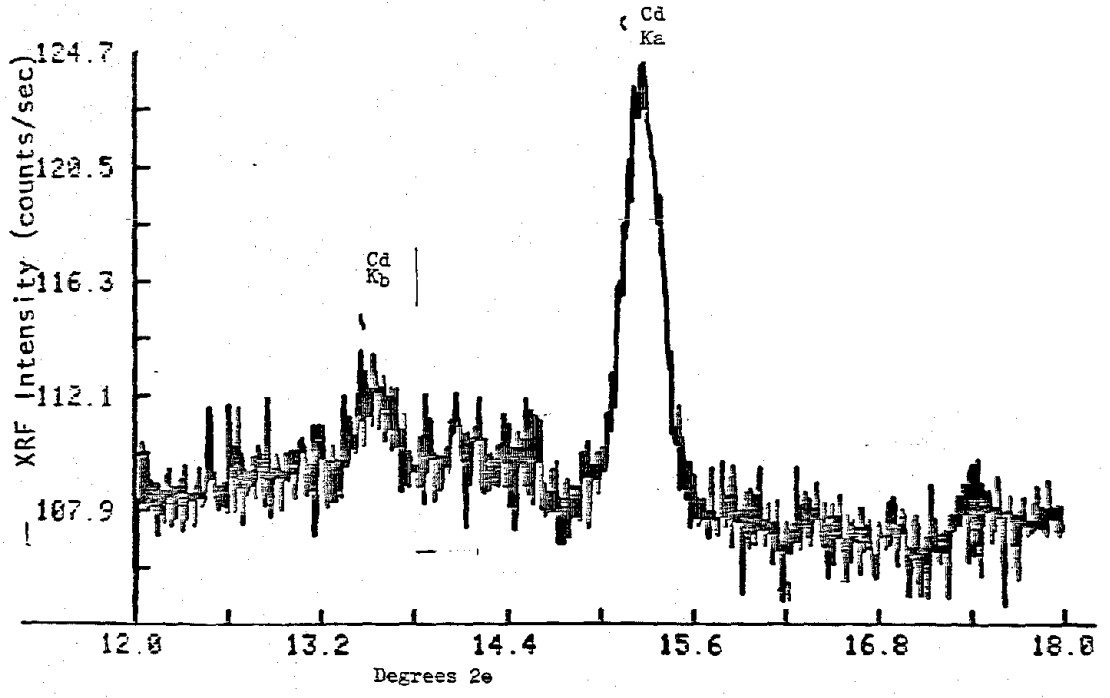

Figure 13. XRF 2e scan of STaFlo-45 brazing fume on AAWP filter.

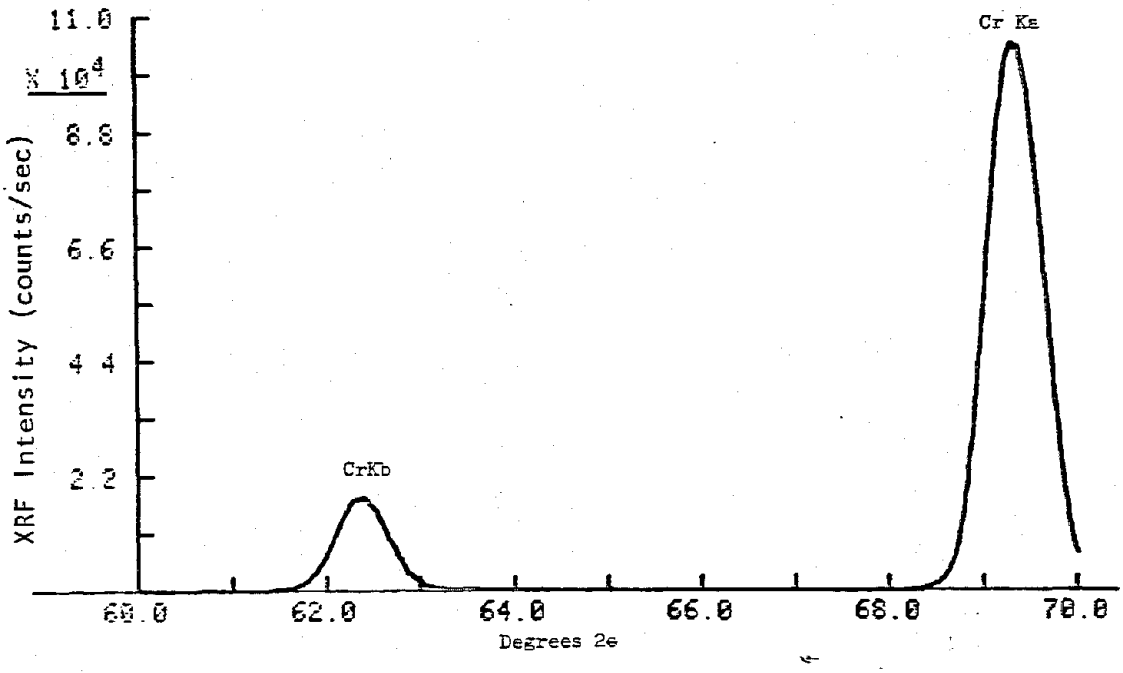

Figure 14. XRF 2e scan of pure chromium metal.

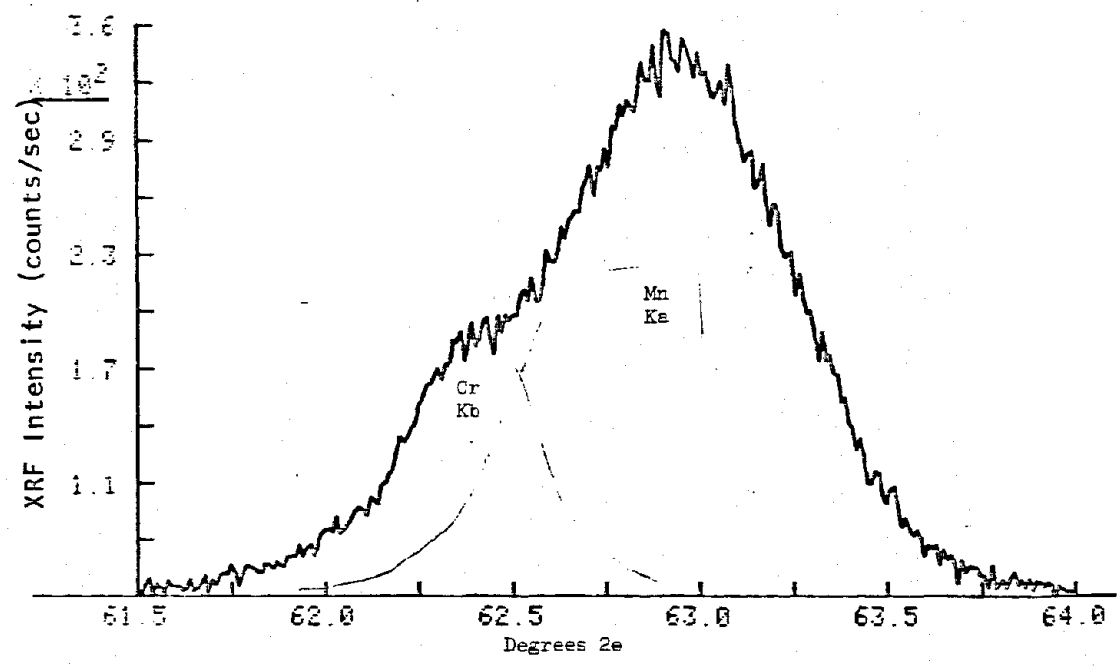

Figure 15. XRF 2e scan of welding fume containing both chromium and manganese, on an AAWP filter.

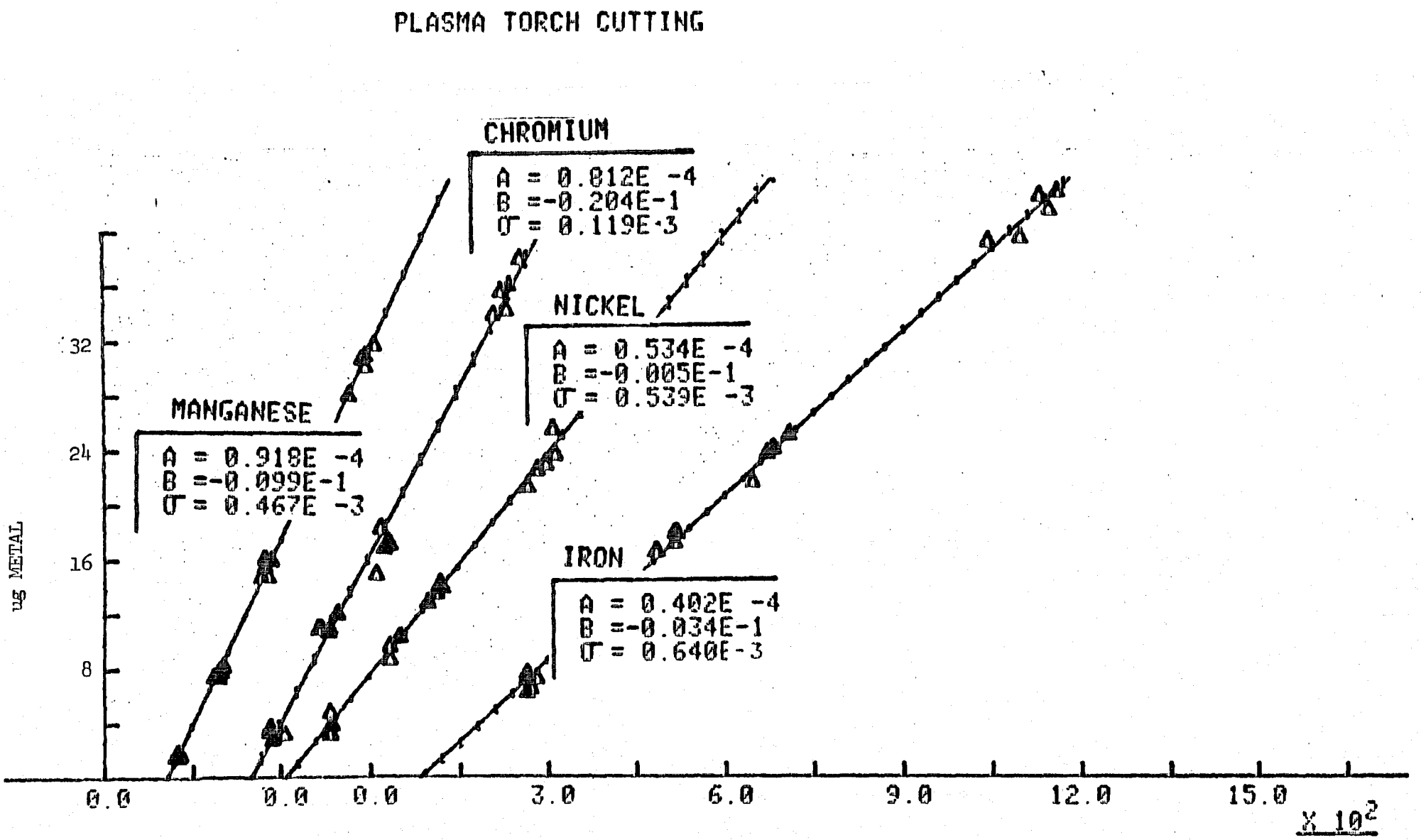

Figure 16. Deposition (by AA) vs, XRF intensity for four metals found in plasma arc cutting fume.

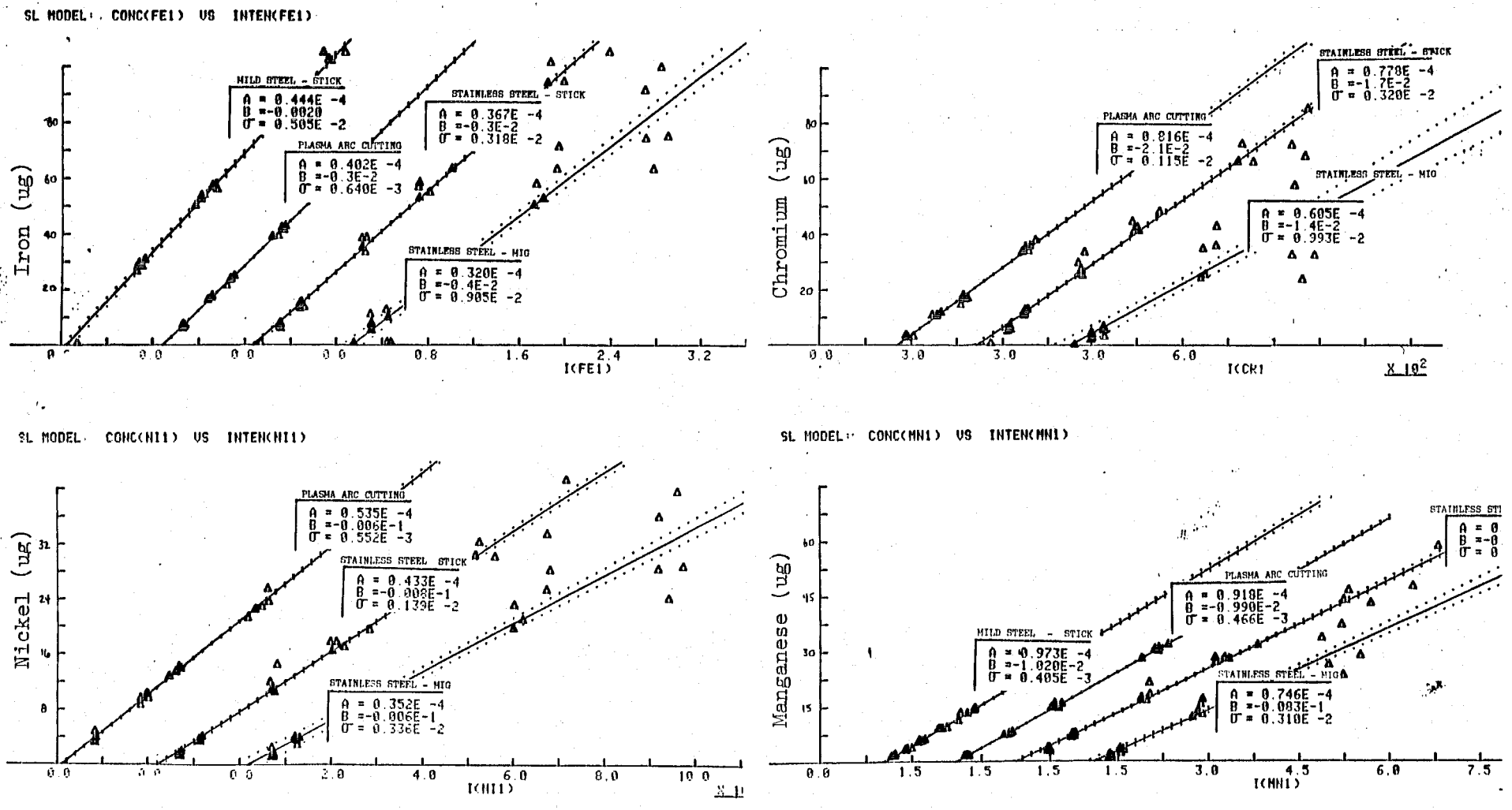

Figure 17. Deposition by AA vs. XRF intensity for iron, chromium, nickel, and manganese by four different welding and cutting processes.

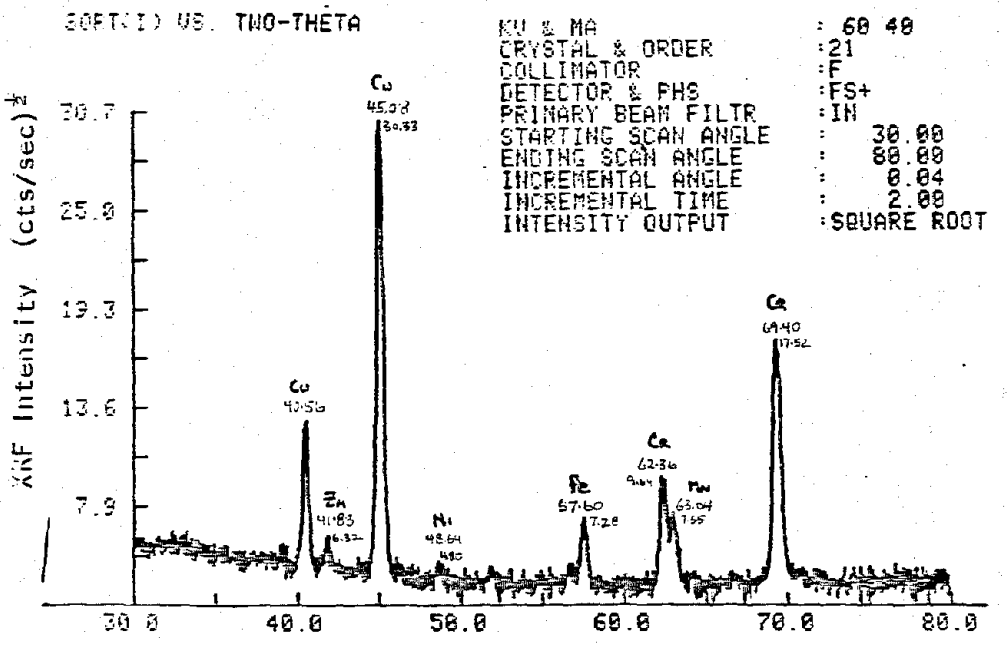

Sample BLANK

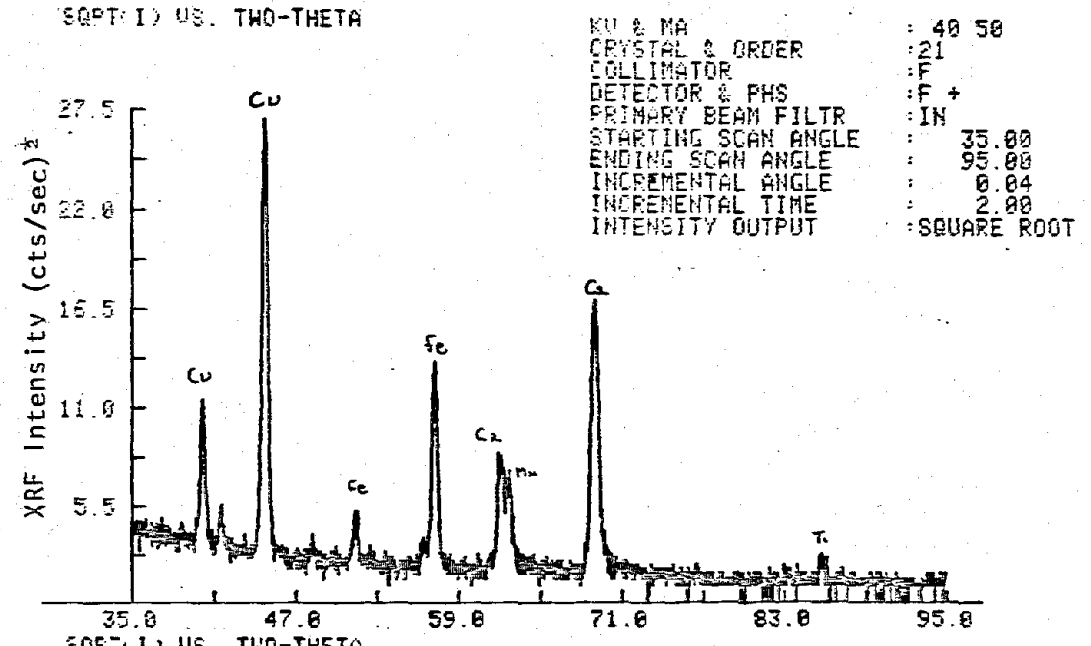

Sample A1

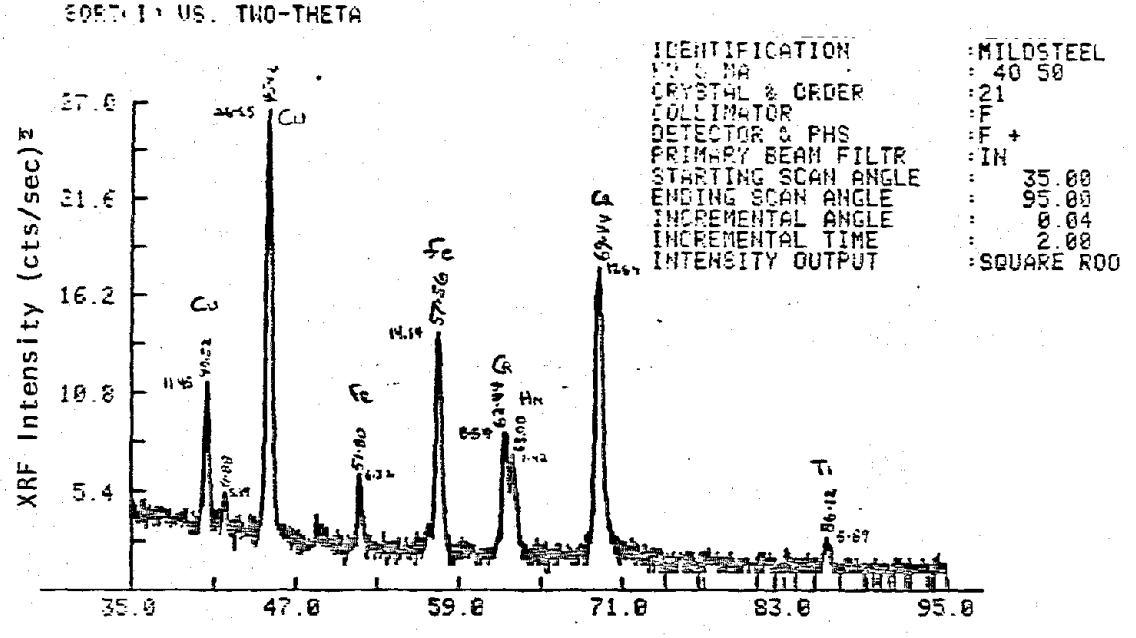

Sample C3

Figure 18. XRF 2e scans of Field Samples, Location 1.

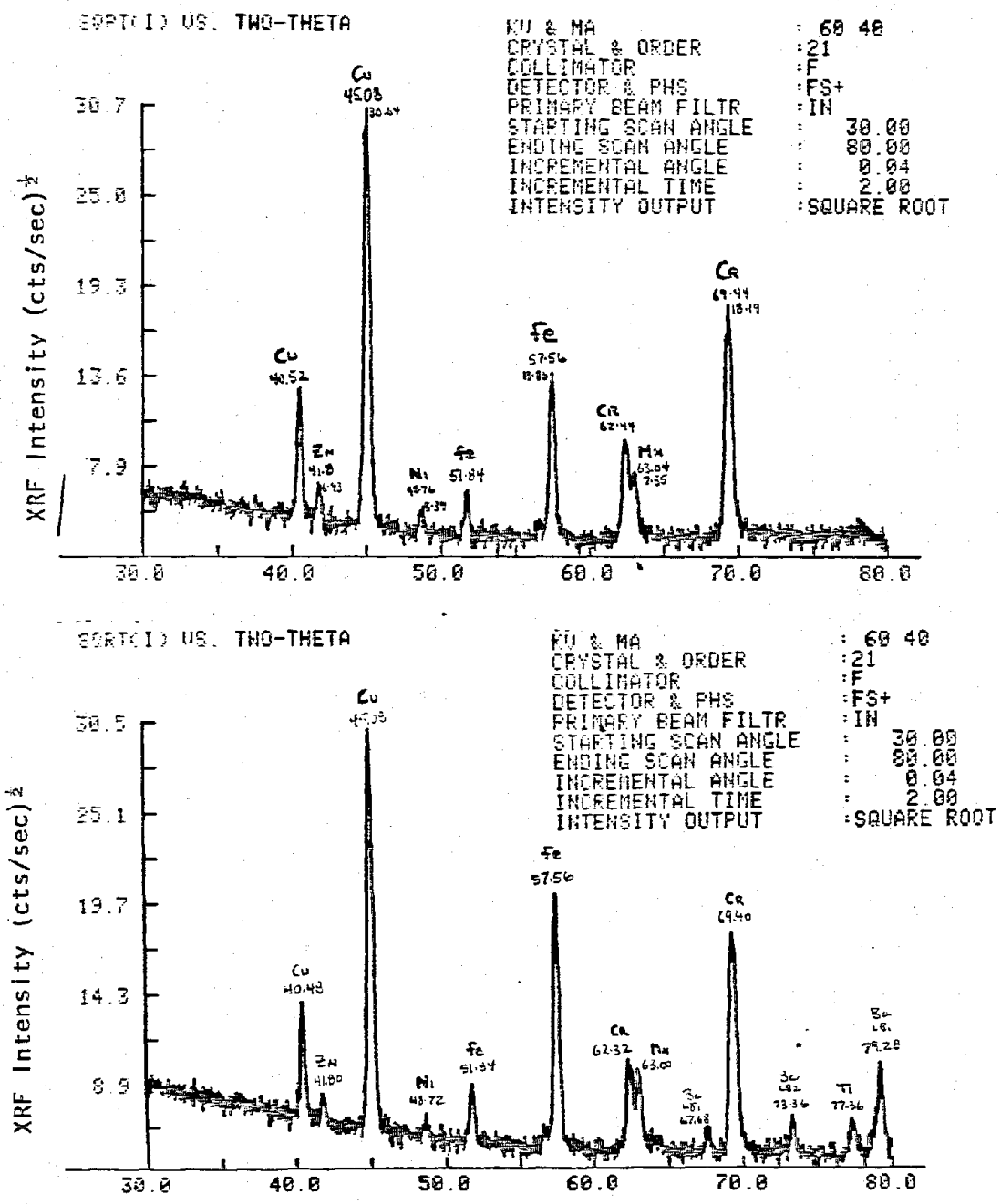

Sample B6

Sample B13

Figure 19. XRF 2θ scans of field samples, location II.

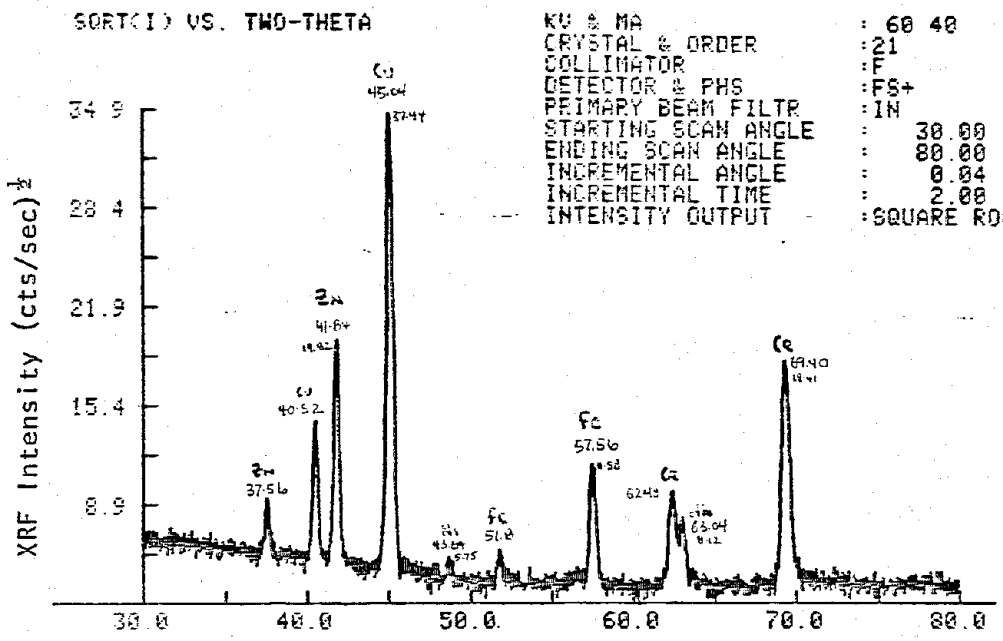

Sample E6

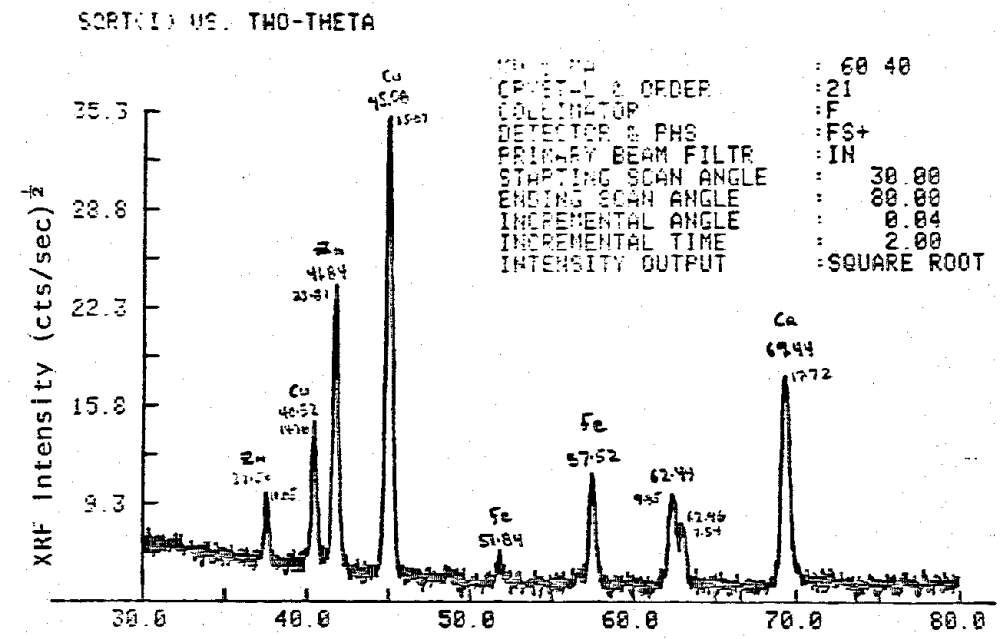

Sample E7

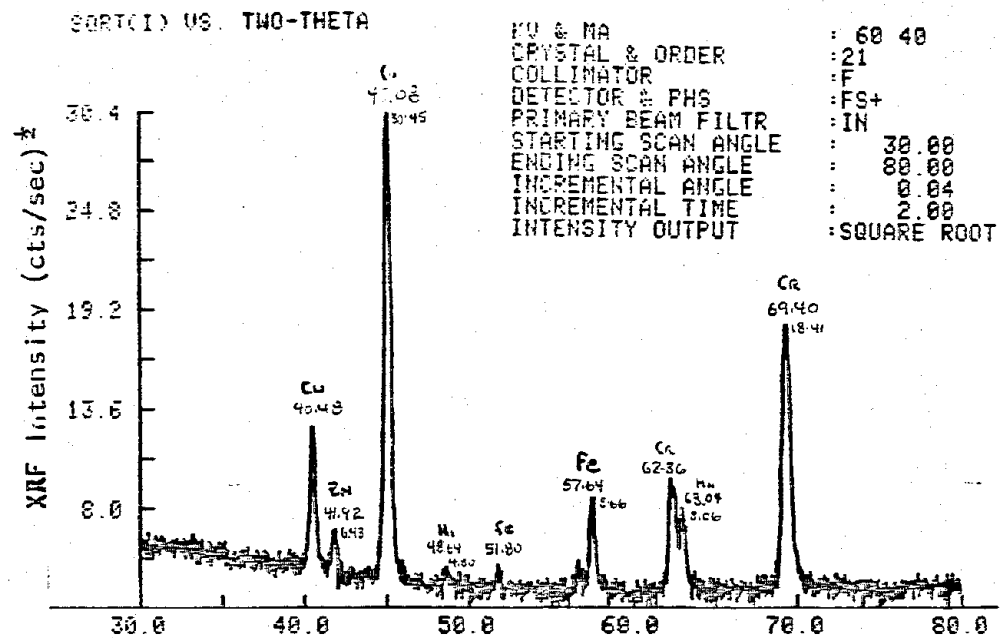

Sample E8.

Figure 20. XRF 2θ scans of field samples

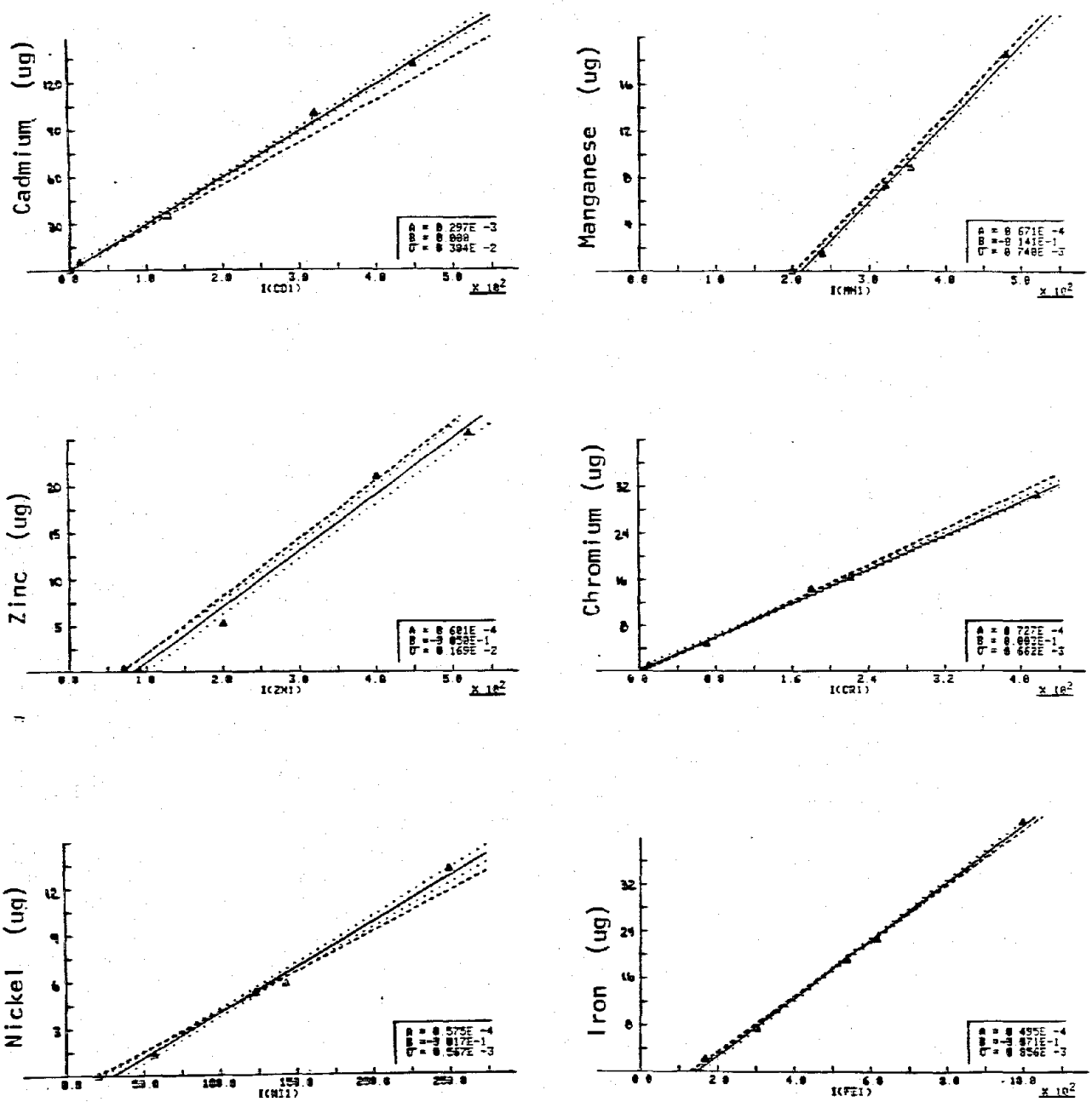

Figure 21. Standard curves for AA-based analysis by XRF. Dashed line is analogous result by ICP. Abcissa unit is XRF intensity in counts per second, ordinate unit is ugm of deposited metal as determined by AA (or ICP).

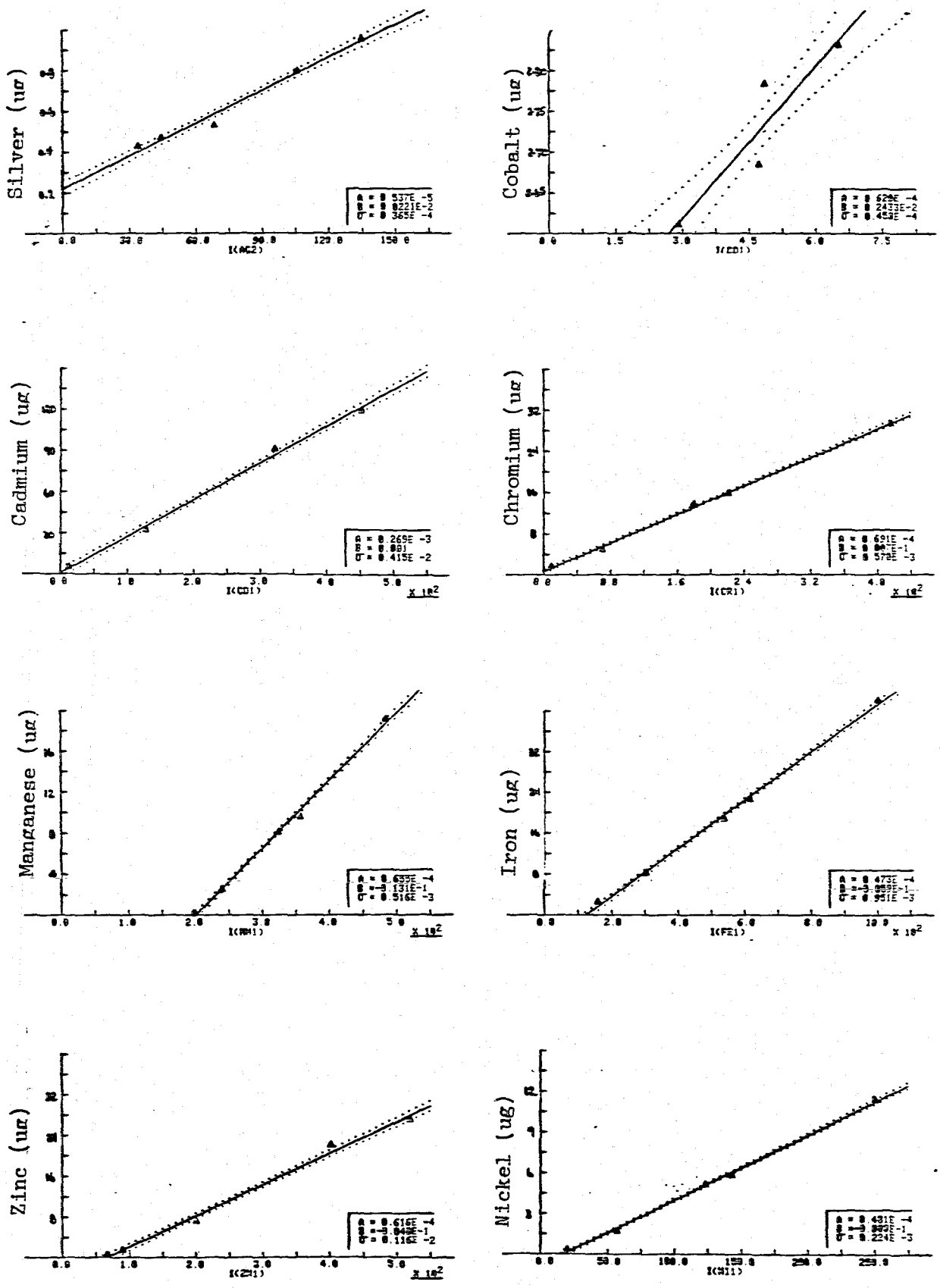

Figure 22. Standard curves for XRF based on ICP analysis.

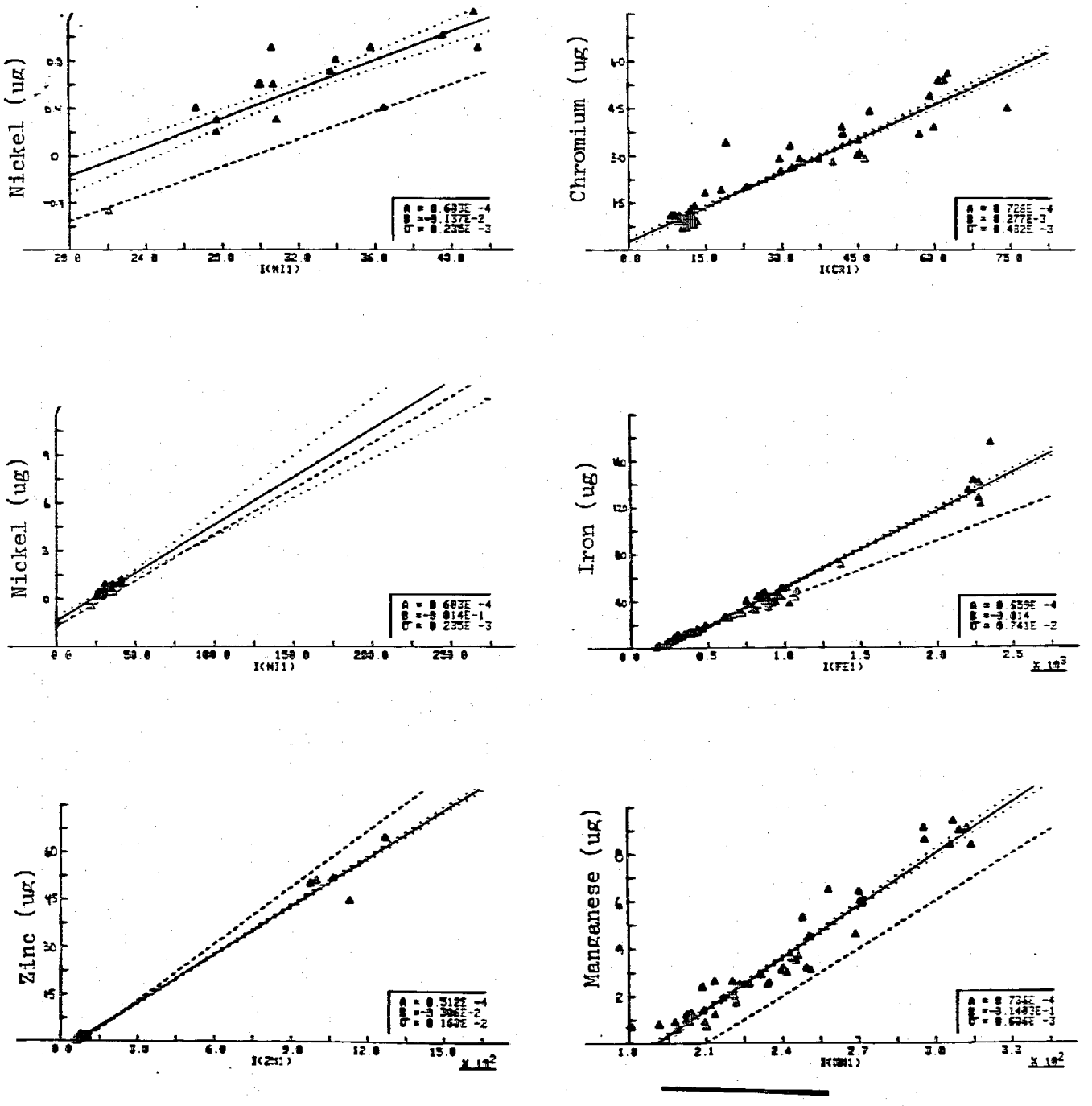

Figure 23. Plots of XRF intensity (abscissa) vs. metal deposition by AA analysis (ordinate). The dashed line is the AA calibration curve; the dotted lines denote the standard deviation of the data.

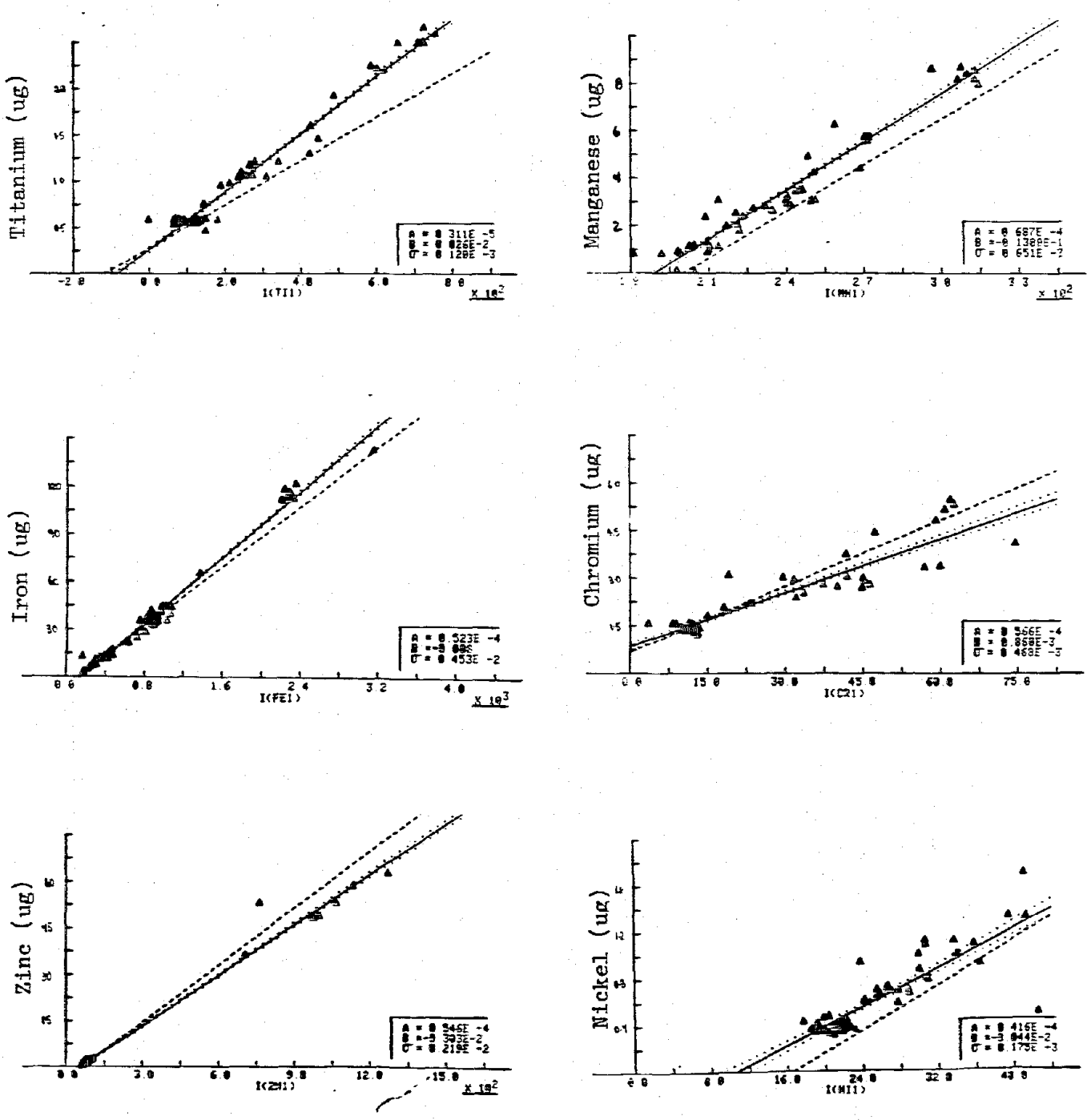

Figure 24. Plots of XRF intensity (abscissa) vs. metal deposition according to ICP analysis (ordinate). The dashed line is the ICP calibration curve. The dotted lines mark the standard deviation of the data.

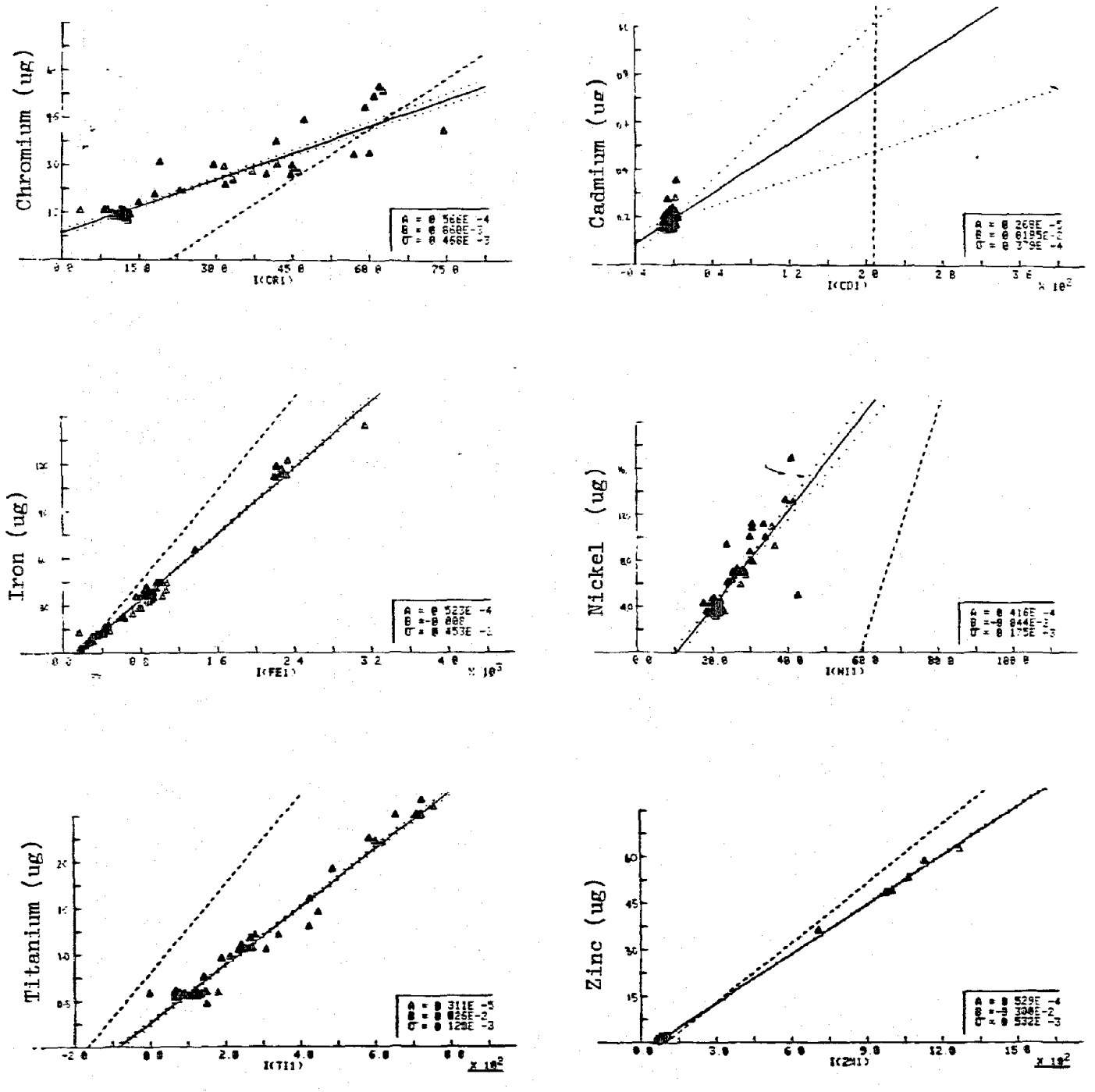

Figure 25. Alternate standardization techniques compared to field sample data (deposition by ICP vs. XRF intensity). The dashed line is the calibration curve based on the XRF analysis of Columbia Scientific type A2 standard filters.

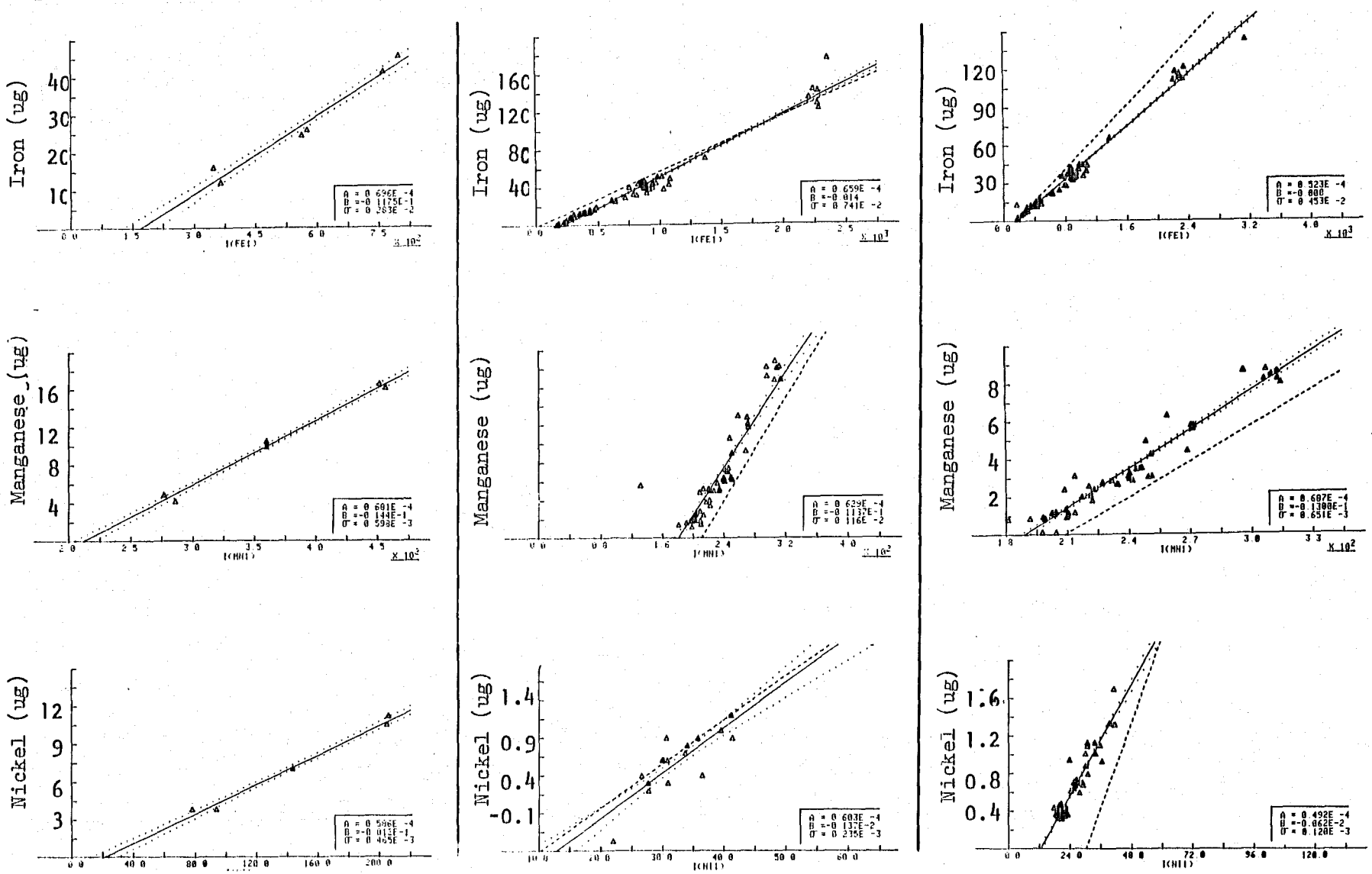

Figure 26. Left column, 26a, calibration curves from Spex multielement standards. Center, 26b, is field samples data by AA, dashed line is Spex calibration curve by AA. Right, 26c, is similar data generated by ICP. Other metals than iron, manganese, and nickel were less successful.

TABLES

Table 1

METALS AND WELDING PROCESSES

METAL NAME	COMPONENTS	WELDING PROCESSES USED
Carbon Steel	Fe, Mn, C	All methods
Low Alloy Steels	Fe, Ni, Cr, C, Mo, V, Si	All methods. Heat treatment may be used.
Stainless Steels: Austenitic:	Fe, C, Cr, Ni, Mo, Mn, Si, P	All methods. Heat treatment may be used.
Chromium Steels:	Fe, Cr, Mg, Mn, Si	SMAW, MIG, TIC, Submerged Arc, Flux-cored arc.
Aluminum and Alloys:	Al, Mn, Mn, Si	Primarily MIG and TIG heat treated.
Nickel and Alloys: Nickel-200:	Ni	SMAC, MIG, TIG
Monel:	Ni-Cu	
Inconel:	Ni-Cr	
Hastelloy:	Ni-Mo-Fe	
Copper and Alloys: Brasses:	Cu-Zn	SMAC, MIG, TIG, Submerged arc
Phosphor bronzes:	Cu-Sn	
Silicon bronzes:	Cu-Si	
Aluminum bronzes:	Cu-Al	
Copper-nickel alloys:	Cu-Ni	
Nickel silvers:	Cu-Zn-Ni	
Beryllium copper:	Cu-Be	
Titanium and alloys:	Ti, Mn, Al, Fe, Cr, Mo	
Lead:	Pb	Oxyacetylene, oxynatural gas, oxyhydrogen flame
Magnezium and alloys:	Mg, Al, Zn, Mn, Zr, Ce, Th, Be, Ca	TIG, MIG, flame, spot

Table 2

Significant Elements in Welding and Brazing Atmospheres
Concentration Ranges

Element	TLV	Range of Method[1]	Observed Range[5]	Resulting Deposition[6]	Detection Limits MDL[7]	MDL[8]	MDL[9]
Al	5mg	0.21–2.1mg/cu m	5 – 28mg/cum	0.6 – 3.4mg	0.135µg	1.35µg	0.01 8µg
As	500µg	420 – 2100µg	–	–	0.10	–	0.06
Be	2µg	4.2 – 8.4µg	0.9 – 4.3µg	0.1 – 0.5mg	–	–	–
Cd	50µg	4.2 – 8.4µg	20 – 270µg	2.4 – 32.4µg	0.02	–	–
Cr	500µg	21 – 210µg	80 – 8000µg	9.6 – 960µg	–	–	0.12
Co	50µg	21 – 210µg	60 – 2400µg	7.2 – 288µg	–	–	0.02
Cu	200µg	21 – 210µg	50 – 2830µg	6 – 340µg	–	0.99	0.26
Fe	5mg	0.021 – 0.210mg	0.1 – 300mg	0.012 – 36mg	0.10	0.92	0.11
Pb	150µg	42 – 840µg	80 – 3500 µg	9.6 – 420µg	0.33	6.15	0.18
Mg	10mg	0.0021–0.021mg	0.08 – 2.92mg	0.01 – 0.35mg	–	–	0.01
Mn	5mg	0.021–0.125mg	0.92 – 14.3mg	0.11 – 1.72mg	–	–	0.09
Mo	5mg	0.625 – 1.65mg	0.02 – 0.143mg	0.0024–0.017mg	–	–	–
Ni	100µg	21 – 210 µg	20 – 640µg	2.4 – 76.8µg	–	–	0.06
Ag	10µg	21 – 170µg	–	–	–	–	–
Sn	2mg	2.4 – 48[2]µmg	0.007 – 0.05mg	0.0008–0.006mg	0.03	–	0.01
Ti	5mg	2.4–25[3]µmg	0.08 – 2.87mg	0.096 – 0.34mg	–	–	0.01
W	1mg	0.06 – 3.9mg[4]	–	–	–	–	–
V	50µg	420 – 6300µg	– 1370µg	– 164.4µg	0.58	0.32	0.04
Zn	5mg	0.0042–0.042mg	1.07 – 60.2mg	0.13 – 7.2mg	0.04	1.11	0.04

1: NIOSH Method 173 unless otherwise specified, 10 mL final solution
2: NIOSH Method 176, colorimetric, 120-L sample
3: NIOSH Method S385, AAS, 120-L sample (linear range)
4: NIOSH Method 271, AAS, 120-L sample
5: From WB TC Draft Criteria Document, per cu.m.
6: 120-L sample
7: "XRF Analysis of Environmental Samples," T. G. Dzubay, Ed., P. 67, for 28 mm spot.
8: J. V. Gilfrich, P. G. Burkhalter, and L. S. Birks, Anal. Chem., 45, 2002 (1973).
9: J. Wagman, R. L. Bennett, K. T. Knapp, "XRF Multispectrometer for Rapid Elemental Analysis of Particulate Pollutans," E.P.A., 1976.

Table 3

Welding and Brazing Processes

Process	Base Metal Composition (%)	Welding Material Nominal Composition (%)
Shielded Metal-Arc (Stick)	Mild Steel, A515 G70 (C: 0.31; Mn: 0.90; P: 0.035; S:0.04; Si: 0.13-0.33; Fe)	6011 Rod (C: 0.09; Mn 0.50; Si: 0.20; P:0.12; S: 0.21; Fe)
Shielded Metal-Arc (Stick)	Stainless Steel, 310 (C: 0.25; Mn: 2.00; P:0.045; S: 0.03; Si: 1.50; Cr: 24-26; Ni: 19-22; Fe)	E310-15 Rod (C: 0.12; Mn: 1.70; Si: 0.4; S: 0.02; P: 0.02; Cr: 26.5; Ni: 21.0; Fe)
Gas Metal-Arc (MIG)	Stainless Steel, 310 (Vida Supra)	310 Wire (C: 0.25; Mn: 2.00; P: 0.045; S: 0.03; Si: 1.50; Cr: 24-26; Ni: 19-22; Fe)
Plasma Arc Cutting	Stainless Steel, 310 (Vida Supra)	—
Brazing	Mild Steel, A515 G70 (Vida Supra)	Easy-Flo 45 (Ag: 45; Cu: 15, Zn: 16; Cd: 24)

Table 4

Summary Of XRD Patterns Of Welding and Brazing Fume Samples

Number	Fume Source	XRD results: 2θ/d/strength/assignment								
1	Stainless steel; MIG	30.2 2.96 m Fe_2O_3 Fe_3O_4	35.55 2.53 s	38.56 2.33 w	43.42 2.08 m	57.31 1.61 m	61.6 1.50 s			
2	Stainless steel; stick	35.375 2.54 s Fe_3O_4 Fe_2O_3 Mn_3O_4	38.58 2.33 w	38.96 2.31 w	43.03 2.10 m	47.07 1.93 m	56.82 1.62 m	61.88 1.50 s Fe_3O_4 Mn_3O_4 Fe_2O_3		
3	Mild Steel; braze	31.61 2.83 m ZnO	32.99 2.71 s CdO	34.33 2.61 m ZnO	36.21 2.48 m ZnO	38.41 2.34 q CdO	55.43 1.66 m CdO	56.58 1.63 w	61.92 1.50 s	66.11 1.41 w
4	Mild steel; stick	35.64 2.52 m	43.59 2.08 w	61.92 1.50 s						
5	Stainless steel; plasma arc cutting	37.59 2.39 w	38.56 2.33 w	43.37 2.09 w	61.86 1.50 s					

Table 5

Instrument Parameter Settings for XRF

	Cr	Mn	Fe	Ni	Zn	Ag	Cd	Sn	Ti	Co
Crystal	2	2	2	2	2	1	2	2	2	2
Collimator	C	C	F	F	F	C	C	C	F	F
Detector	F	F	F	F	FS	F	FS	F	F	F
PHS	25,35	30,28	33,25	35,25	30,50	20,35	36,00	30,30	15,35	32,38
Peak 2θ	69.36	62.97	57.52	48.67	41.80	56.74	15.28	126.77	86.14	52.80
Background 2θ	70.50	61.00	58.50	50.00	43.00	56.00	14.60	124.50	87.5	53.5

Key:
1. All Kv = 60, Ma = 40, Cr Kx X-ray tube utilized. All intensities measured for 100 seconds.
2. Crystal 2 = L.F - 200; Crystal 1 - PET
3. Callimator: C = Course, F = Fine
4. Detector: F = Flow counter, S = Scintillation counter
5. PHS = Pulse height selector. First number is baseline, second is window.
6. Background intensities are subtracted from Peak 2θ intensities without modification except for Cd, where a factor of 0.946 was used to account for the slope in the backgound intensity.
7. A main beam filter was used for chromium and manganese

Table 6

Typical Analytical Results: Plasma Arc Cutting Fume Samples

	IRON						NICKEL						CHROMIUM						MANGANESE					
	AA (μg)	ICP (μg)	Δ	Bias	t-test	XRF CTS/SEC)	AA	ICP	Δ	Bias	t-test	XRF CTS/SEC	AA	ICP	Δ	Bias	t-Test	XRF	AA	ICP	Δ	Bias	t-Test	XRF
VL	7.02	7.02	0	0.00	3.207	268.6	3.9	3.12	0.78	0.20	2.735	84.6	3.26	4.34	-1.08	-33.12	2.332	293.3	1.7	2.02	-0.32	-18.24	5.488	126.58
RSD	7.76	7.22				2.63	15.8	8.30				1.79	9.84	22.84				3.67	7.2	7.34				2.15
L	17.26	17.18	0.08	0.46	4.00	502.3	9.8	8.24	1.56	15.92	7.150	194.6	11.18	11.74	-0.56	-0.05	5.199	3.31	7.8	7.12	0.68	8.71	3.207	195.16
RSD	3.77	4.06				3.62	6.73	4.08				4.56	5.23	3.74				3.41	4.62	2.49				2.62
M	23.78	23.74	0.04	0.17	3.207	676.6	13.7	11.20	2.5	18.25	10.624	263	16.9	17.52	-0.62	-0.04	3.206	476	15.5	15.24	0.26	1.68	3.302	273.1
RSD	5.38	5.99				3.35	3.96	5.75				3.62	7.06	7.34				1.76	4.26	4.97				2.39
H	41.22	41.78	-0.56	-1.36	5.136	1113.2	23.26	19.62	3.64	15.65	5.358	447	35.64	35.86	-0.22	-0.01	4.332	684.4	30.36	29.88	0.48	1.58	1.784	439.8
RSD	4.24	4.01				4.15	6.76	4.48				4.39	4.60	5.20				2.46	4.58	4.34				3.57
Average			-0.11	-0.18	3.888				2.120	17.45	6.467				-0.055		10.61	3.892			0.275	-1.71	3.445	
Corr						>0.999						>0.999						>0.997						>0.999

Key: Δ = AA-ICP in μg/Filter, average of five samples at each level
Bias = Δ/AA x100
t-Test = 2.776 denotes significant difference between AA and ICP analytical results
Data truncated to four significant figures.

Table 7

Welding and Brazing Field Sample Data

Location	Designation	Type	Location Description	Time
I	A1-A3	Area	Top of partition between welding booths, 8 feet from floor, near vent. fan.	45 Min
	B1-B6	Area	Same as above but between different booths	20 Min
	C1-C6	Area	Same as above but quite close to vent. fan.	22 Min
	D1-D3	Personal	Inside welders helmet, near nose	15 Min
II	E1-E6	Area	Near welder using galvanized and sheet metal carbon are welding	30 Min
	E7	Personal	Inside helmet of above welder	30 Min
	E8-E9	Personal	Inside helmet, welding using stainless steel (308) stick welding	30 Min
	E10-15	Area	In vicinity of above welding	33 Min
III	F1-F16	Personal	Operator of automatic welding # 1	30 Min
	F2-F17	Personal	Operator of automatic welding # 2	30 Min
	F3-F8	Area	15 Feet from two automatic welding machines	83 Min
	F9-F14	Area	Near one automatic welder (2 Lpm flow limiting orifaces	88 Min
	F15-F18	Personal	Inside helmet of welding using carbon-steel stick welding (7818 rods) on 308 stainless steel	30 Min

* Pandjaris automated MIG Scamer-Welding, using 75% He/25% Ar on type 304 1/4" or 3/8" Stainless Steel

Table 8

Calibration Data for the X-Ray Fluorescence Analysis of Welding and Brazing Fumes

ICP CALIBRATION DATA

	ELEMENT	INTEN	CONC(µg)
	AG2	44.6	0.5
	CD1	12.6	5.2
	CO1	2.9	2.6
VL	CR1	70.0	5.0
	FE1	306.0	8.2
	MN1	240.5	2.6
	NI1	57.4	1.7
	SI1	87.4	16.4
	SN2	0.0	1.0
	TI1	84.0	0.5
	ZN1	90.6	1.5
	AG2	68.2	0.5
	CD1	129.0	32.9
	CO1	4.7	2.7
	CR1	180.3	13.9
	FE1	540.6	18.9
L	MN1	325.0	8.0
	NI1	123.7	5.2
	SI1	122.9	15.8
	SN2	3.9	0.9
	TI1	133.0	0.6
	ZN1	200.7	7.2
	AG2	106.0	0.8
	CD1	322.0	92.0
	CO1	4.8	2.8
	CR1	221.7	15.9
	FE1	617.3	22.7
M	MN1	357.6	9.6
	NI1	143.7	5.9
	SI1	102.0	11.9
	SN2	4.7	0.9
	TI1	137.3	0.6
	ZN1	403.0	2.3
	AG2	135.0	0.9
	CD1	452.0	120.2
	CO1	6.5	02.8
	CR1	417.3	29.6
	FE1	1002.0	42.2
H	MN1	486.3	19.2
	NI1	251.0	11.4
	SI1	184.0	11.9
	SN2	4.4	1.0
	TI1	160.7	0.6
	ZN1	521.0	27.3

AA CALIBRATION DATA

	ELEMENT	INTEN	CONC(µg)
	CR1	70.0	4.8
	MN1	239.3	1.5
	FE1	306.0	7.4
VL	NI1	57.4	1.3
	ZN1	90.6	0.2
	CD1	12.5	5.3
	CR1	180.3	14.4
	MN1	322.1	7.4
L	FE1	540.6	19.2
	NI1	123.6	5.3
	ZN1	200.6	5.2
	CD1	129.0	35.1
	CR1	221.6	16.3
	MN1	354.1	8.9
M	FE1	617.3	22.7
	NI1	143.6	5.9
	ZN1	403.0	21.0
	CD1	322.0	100.7
	CR1	417.0	30.4
	MN1	479.7	18.6
	FE1	1002.0	43.0
H	NI1	251.0	13.1
	ZN1	523.0	25.7
	CD1	451.0	131.5
	CR1	9.1	1.0
	MN1	198.8	0.0
BL	FE1	168.0	2.1
	NI1	20.7	0.0
	ZN1	70.5	0.4
	CD1	0.0	0.0
	AG2	34.3	0.4
	CD1	0.0	0.2
	CO1	3.0	2.7
	CR1	9.2	1.7
	FE1	161.0	2.7
BL	MN1	197.0	0.2
	NI1	19.8	0.4
	SI1	29.7	11.9
	SN2	4.7	1.1
	TI1	59.0	0.5
	ZN1	66.4	0.4

Table 9

Comparison of metal fume concentrations by AA and by XRF using the AA calibration curve of Figure 21. Location I Field Samples. mg/m^3

	Fe		CR		MA		ZN	
	AA	XRF	AA	XRF	AA	XRF	AA	XRF
1A	0.709	0.809	0.0	0.004	0.057	0.035	0.0	0.0
2A	0.738	0.857	0.002	0.004	0.062	0.043	0.0	0.0
3A	0.889	0.950	0.0	0.007	0.067	0.059	0.0	0.0
1B	1.761	1.771	0.0	0.015	0.152	0.098	0.0	0.0
2B	1.790	1.605	0.0	0.009	0.148	0.093	0.0	0.0
3B	1.834	1.820	0.0	0.015	0.156	0.127	0.0	0.0
4B	1.979	1.807	0.0	0.009	0.163	0.107	0.0	0.0
5B	1.826	1.343	0.005	0.000	0.134	—	0.005	0.0
1C	6.244	4.514	0.004	0.009	0.418	0.289	0.0	0.0
2C	7.254	4.499	0.0	0.008	0.382	0.285	0.0	0.0
3C	5.854	4.435	0.0	0.009	0.373	0.284	0.0	0.0
4C	5.101	4.405	0.004	0.008	0.382	0.280	0.0	0.0
5C	5.445	4.611	0.0	0.009	0.374	0.296	0.0	0.0
6C	6.181	4.603	0.004	0.004	0.406	0.258	0.0	0.0
D1	3.093	2.921	0.0	0.020	0.204	0.132	0.0	0.0
D2	2.984	2.235	0.0	0.006	0.090	0.092	0.033	0.0
D3	3.224	2.598	8.0	0.0	0.244	0.158	0.0	0.0

Table 10

Comparison of metal fume concentrations by AA and by XRF using the AA calibration curve of Figure 21. Location II field samples. (mg/m^3)

	FE		CR		MN		ZN	
	AA	XRF	AA	XRF	AA	XRF	AA	XRF
E1	0.168	0.173	0.003	0.0	0.020	0.0	0.977	0.947
E2	0.317	0.300	0.002	0.0	0.024	0.0	1.243	1.324
E3	0.340	0.302	0.007	0.005	0.033	0.0	1.304	1.481
E4	0.353	0.341	0.002	0.004	0.034	0.0	1.096	1.538
E5	0.322	-	0.003	0.0	0.0	-	1.032	-
E6	0.363	0.312	0.003	0.005	0.033	0.0	1.280	1.364
E7	0.385	0.319	0.003	0.003	0.038	0.0	2.044	2.243
E8	0.037	0.063	0.028	0.019	0.038	0.006	-	0.0
E9	0.109	0.093	0.061	0.048	0.064	0.022	0.010	0.0
E10	0.319	0.232	0.110	0.082	0.145	0.087	0.045	0.003
E11	0.317	0.289	0.122	0.106	0.110	0.114	0.039	0.017
E12	0.310	0.304	0.133	0.113	0.186	0.116	0.041	0.011
E13	0.291	0.274	0.124	0.107	0.167	0.116	0.043	0.005
E14	0.295	0.248	0.114	0.105	0.155	0.073	0.041	0.0
E15	0.291	0.168	0.085	0.071	0.106	0.065	0.047	0.005

Table 11

Comparison of metal fume concentrations by AA and by XRF using the AA calibration curves of Figure 21. Location III field samples. (mg/m^3)

	Fe		Cr		Mn		Zn		Ni	
	AA	XRF	AA	XRF	AA	XRF	AA	XRF	AA	XRF
F1	0.182	0.129	0.031	0.031	0.060	0.013	0.003	0.0	0.009	0.0
F2	0.356	0.288	0.072	0.050	0.265	0.217	0.009	0.0	0.013	0.0
F3	0.320	0.313	0.024	0.031	0.011	0.0	0.008	0.0	0.005	0.005
F4	0.261	0.250	0.018	0.018	0.007	0.0	0.007	0.0	0.003	0.0
F5	0.143	0.352	0.031	0.040	0.010	0.0	0.008	0.0	0.018	0.007
F6	0.275	0.240	0.021	0.020	0.008	0.0	0.006	0.0	0.007	0.0
F7	0.425	0.384	0.040	0.053	0.008	0.0	0.009	0.001	0.014	0.007
F8	0.368	0.354	0.034	0.044	0.008	0.0	0.008	0.004	0.012	0.006
F9	0.263	0.200	0.016	0.014	0.014	0.0	0.011	0.0	0.005	0.0
F10	0.292	0.243	0.015	0.015	0.015	0.001	0.004	0.0	0.004	0.001
F11	0.237	0.193	0.010	0.013	0.015	0.003	0.003	0.0	0.003	0.0
F12	0.254	0.192	0.011	0.012	0.014	0.009	0.004	0.0	0.003	0.0
F13	0.231	0.201	0.011	0.016	0.015	0.005	0.004	0.0	0.005	0.001
F14	0.210	0.108	0.011	0.013	0.013	0.006	0.003	0.001	0.005	0.002
F15	0.537	0.452	0.012	0.009	0.028	0.0	0.0	0.0	0.0	0.0
F16	0.349	0.374	0.047	0.047	0.145	0.123	0.003	0.0	0.006	0.0
F17	0.205	0.109	0.025	0.013	0.054	0.022	0.006	0.0	0.0	0.0
F18	0.115	0.818	0.073	0.022	0.201	0.099	0.009	0.0	0.0	0.0

Table 12

Summary of Field Sample Analyses

	IRON		CHROMIUM		MANGANESE		NICKEL		ZINC	
	AA	ICP	AA	ICP	AA	ICP	AA	ICP	AA	ICP
Location I										
Δ (mg/m^3)	0.654	0.257	-0.007	-0.007	0.071	0.04	*	+0.008	*	0.021
t-Test for Δ	3.363	3.195	4.619	4.343	7.156	4.823	*	2.526	*	6.454
t(95% Sig.)	2.567	2.567	2.567	2.567	2.583	2.583	*	2.583	*	2.567
Bias (%)	14.47	3.41	*	-13.04	31.54	4.19	*	36.47	*	*
Location II										
Δ (mg/m^3)	0.036	0.015	0.01	0.133	0.04	0.026	*	0.007	-0.06	-0.062
t-Test for Δ	3.618	2.147	3.761	2.428	9.332	8.502	*	7.579	1.392	1.610
t(95% Sig.)	2.634	2.650	2.624	2.624	2.624	2.650	*	8.650	2.650	2.624
Bias (%)	13.10	3.18	10.15	4.38	45.58	*	*	*	-10.84	-10.01
Location III										
Δ (mg/m^3)	0.046	-0.008	0.002	-0.006	0.02	0.012	0.00	0.003	0.01	0.003
t-Test for Δ	2.786	0.511	0.599	2.422	3.858	2.972	5.277	5.592	7.949	4.225
t(95% Sig.)	2.562	2.567	2.552	2.567	2.552	2.567	-2.552	-2.567	-2.552	-2.567
Bias (%)	12.82	- 4.53	12.21	-24.24	*	*	*	*	*	*
Average										
Δ	0.245	0.088	0.002	0.04	0.044	0.026	*	0.006	-0.03	-0.013
Bias	13.46%	0.69%	11.18	-10.97	38.56	*	*	*	*	*

* Many Near-zero depositions interfere with calculation of these data entries

Key: Δ = (AA deposition)-(XRF deposition)/(AA deposition) or with ICP deposition

Bias = Δ/(AA deposition) or similarly for ICP deposition

t-Test by $t = \frac{\bar{X}\sqrt{n}}{\sigma}$ where $\bar{X}$ = Average of differences, AA-XRF (Δ)
N = Number of samples at a location
σ = Standard deviation of difference

Table 13

SUMMARY OF ANALYSIS DATA

Metal	Location	Sample Numbers	Bias (%)	Δ (mg/m^3)	T-Test for Δ
Iron	I	All	14.47 %	0.654	3.363
Iron	II	All	13.10 %	0.036	3.618
Iron	III	All	12.82 %	0.046	2.786
Manganese	I	All	31.54 %	0.071	7.156
Zinc	II	1-4, 6-7	-12.27%	-0.159	1.392
Chromium	II	8-15	18.14%	0.016	7.153
Chromium	III	All	12.21%	0.002	0.599
Average			12.86%	0.095 mg/m^3	

APPENDICES

APPENDIX I

Table 1

Summary of Field Sample Data, AA Results (μg / filter)

	IRON	CHROMIUM	MANGANESE	NICKEL	ZINC
Location I					
Δ = AA- XRF	13.459	-0.218	1.563		0.276
T-test for Δ °	2.871	3.906	7.618		5.933
T(99% Sig.)	2.898	2.898	2.921		2.878
Bias ($\frac{AA-XRF}{AA}$)	13.99%	-18.75%	32.09%	*	*
Location II					
Δ = AA - XRF	1.100	0.300	1.540		-2.223
T-test for Δ	1.542	4.088	14.192		1.415
T(99% Sig.)	2.977	2.977	2.977		2.650
Bias ($\frac{AA-XRF}{AA}$)	10.04%	8.78	39.70% (10-15)	*	-10.86% (1-7)
Location III					
Δ = AA-XRF	3.928	-0.300	1.400	0.389	0.92
T-Test for Δ	4.380	1.084	7.971	6.165	9.656
T(99% Sig.)	2.898	2.898	2.898	2.898	2.898
Bias ($\frac{AA-XRF}{AA}$)	11.50%	-2.65%	58.66%	*	*
Averages					
Δ	6.162	-0.073	1.501		-0.342
Bias	11.84%	-2.44%	43.48%	*	*

° $T = \frac{\bar{X}\sqrt{N}}{\sigma}$ where $\bar{X}$ = Average difference (Δ), N = numbers of samples, σ = std deviation (Laitinen, p. 549)

* designates too little meaningful data to compute a particular entry

Appendix I

Table 2

Summary of Field Sample Data, ICP Results (μg/filter)

	IRON	CHROMIUM	MANGANESE	NICKEL	ZINC	CADMIUM	COBALT	TRANIUM
Location I								
Δ = ICP - XRF	4.645	-0.18	0.763	0.158	0.455	-0.247	-0.240	0.535
T-test for Δ	2.597	6.990	4.224	3.002	11.179	2.127	4.486	6.139
T(99% Sig.)	2.861	2.861	2.878	2.878	2.861	2.878	2.861	2.861
Bias	3.41%	-13.04%	4.19%	36.47*	*	*	-10.03%	*
Location II								
Δ = ICP - XRF	0.529	0.133	0.907	0.236	-5.257	-0.200	-0.071	0.440
T-test for Δ	2.159	2.428	8.904	7.664	1.922	1.259	2.347	4.631
T(99% Sig.)	3.012	2.979	3.012	3.012	3.707	2.977	3.012	2.977
Bias	3.18%	4.66%	*	*	-10.01%	*	-2.83%	*
Location III								
Δ = ICP - XRF	-0.263	-0.721	0.700	0.226	0.253	-0.021	-0.422	-0.011
T-Test for Δ	0.378	4.821	3.618	4.943	3.011	0.221*	3.262	0.356
T(99% Sig.)	2.878	2.878	2.878	2.878	2.878	2.878	2.898	2.898
Bias	-4.53%	-24.24%	*	*	*	*	-12.56%	*
Averages								
Δ	1.637	-0.256	0.790	0.207	-1.516	-0.156	-0.197	0.321
Bias	0.69%	-13.13%	14.19%	*	*	*	-8.47%	*

*Many near-zero depositions interfere with calculations of these entries

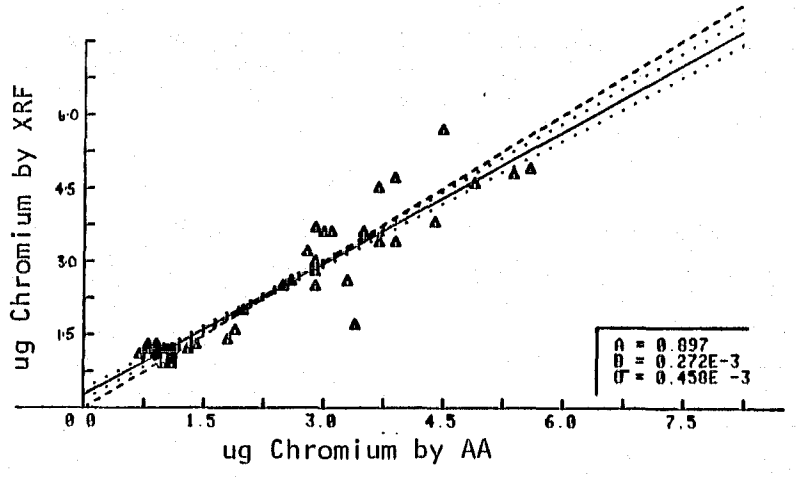

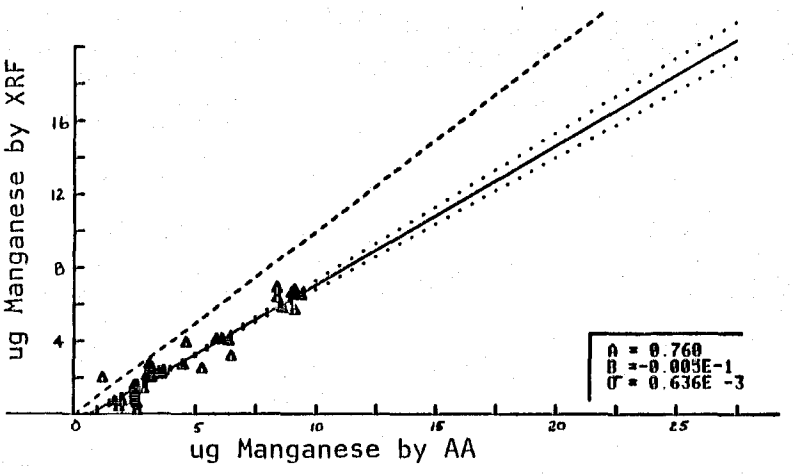

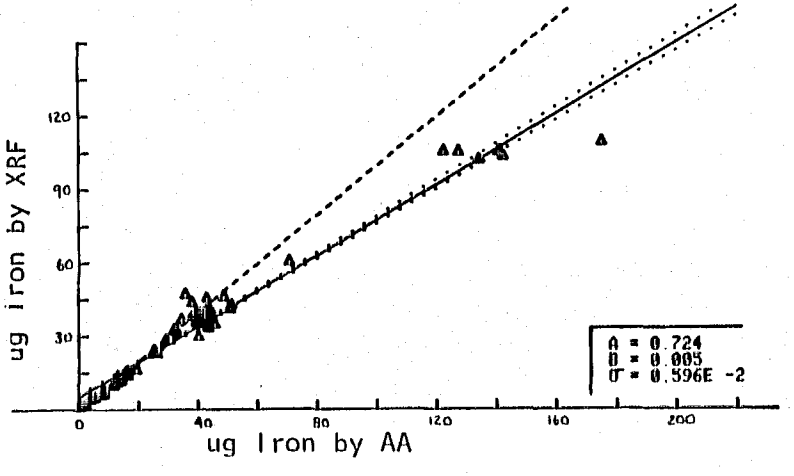

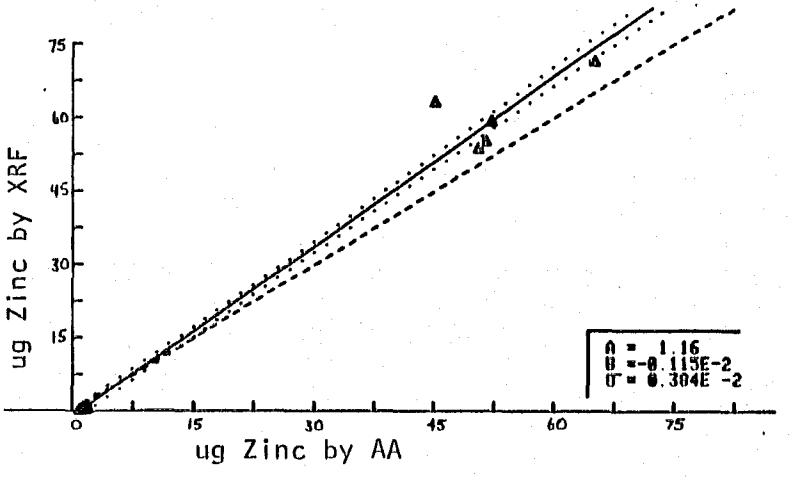

Appendix 2, Figure 1. Comparison of metal depositions calculated by XRF, AA calibration (ordinate), and by AA (abscissa), for the field samples of welding and brazing fumes. The solid line is the least squares fit of the data; dotted lines bracket the standard deviation; the dashed line is the slope = 1 (45°) denoting exact equality of the two sets of calculated results.

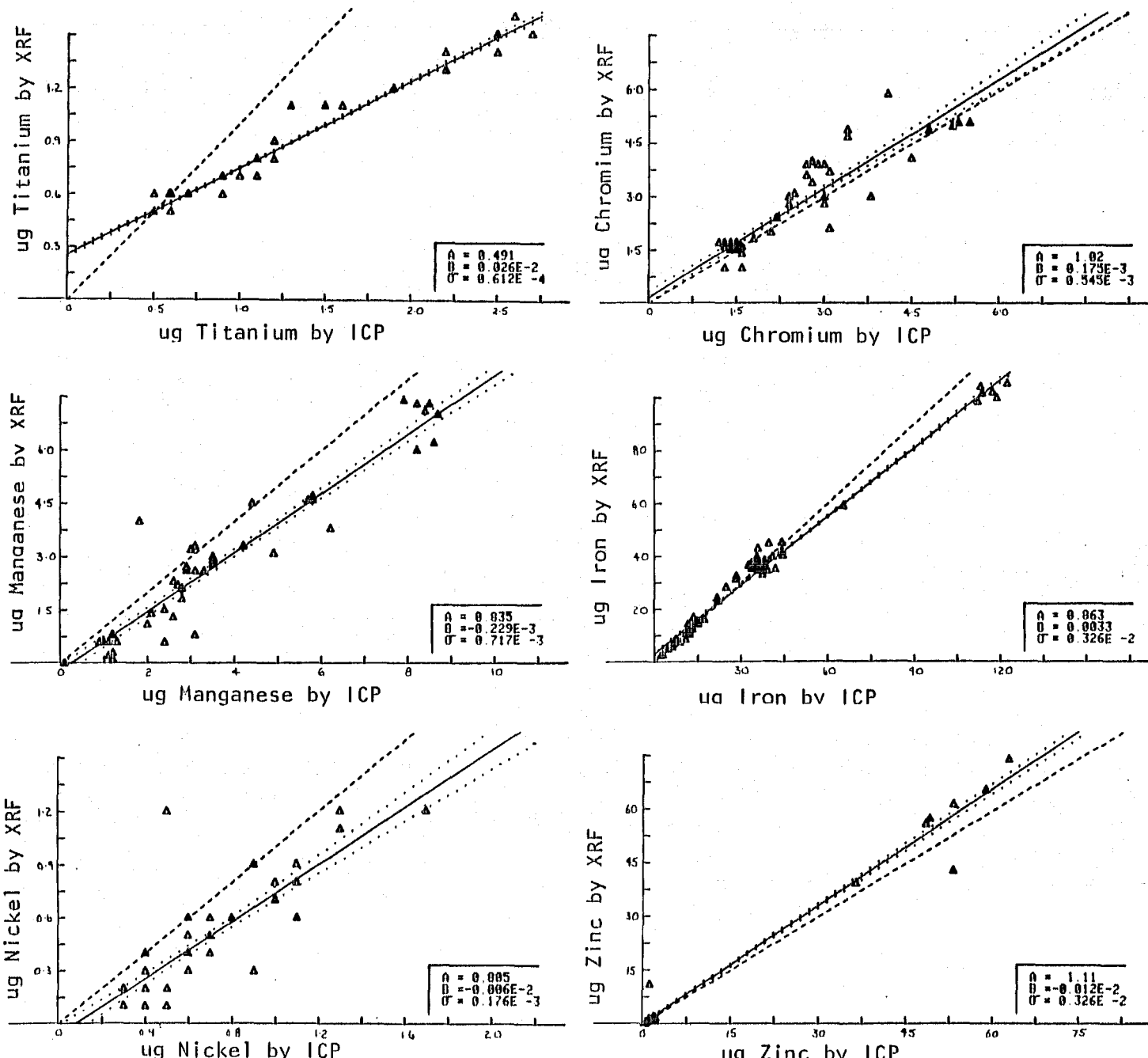

Appendix 2, Figure 2. Comparison of metal depositions calculated by XRF [ICP calibration], ordinate, and by ICP, abscissa. The solid line is the least squares fit: dotted lines bracket the standard

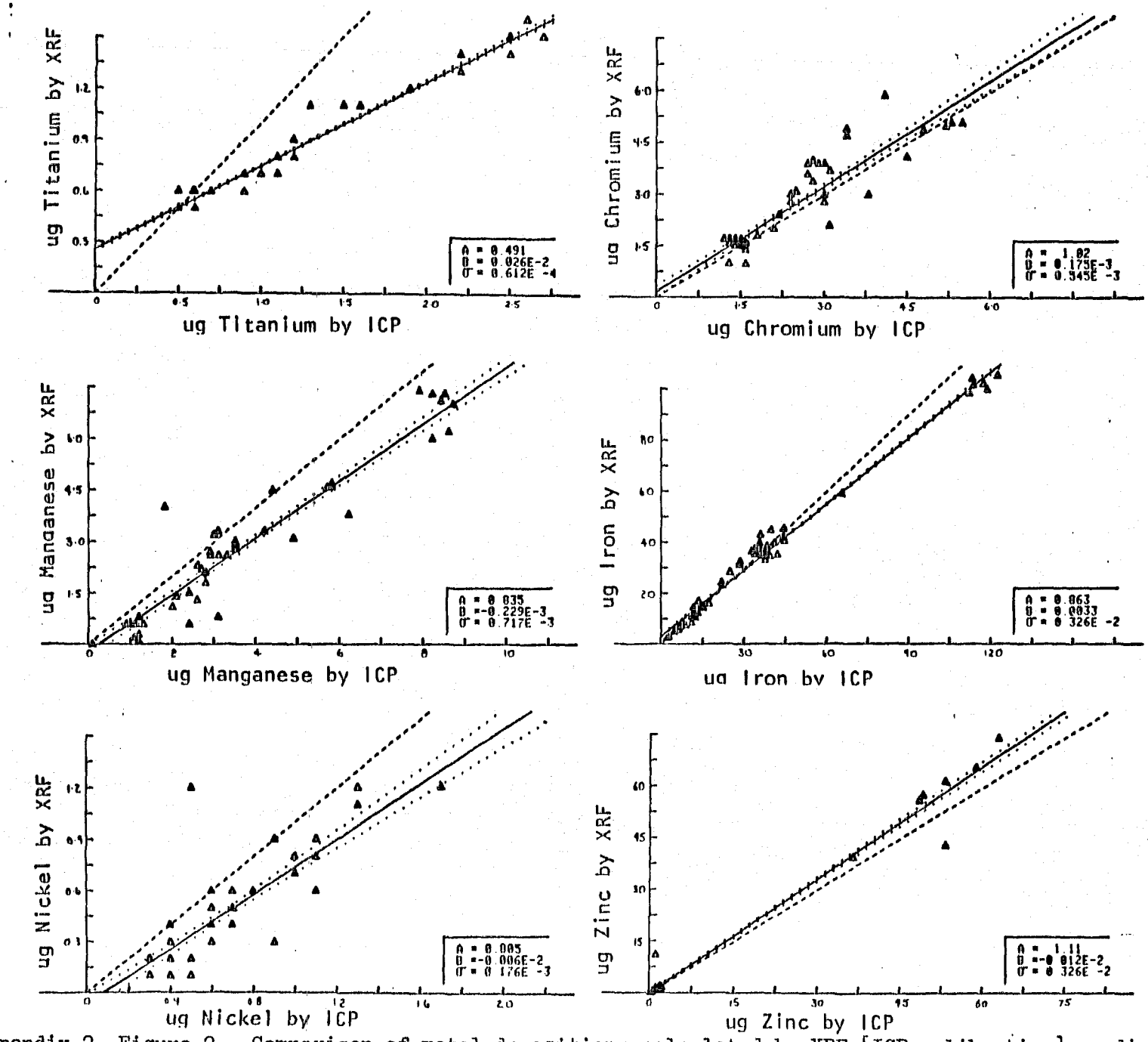

Appendix 2, Figure 2. Comparison of metal depositions calculated by XRF [ICP calibration], ordinate, and by ICP, abscissa. The solid line is the least squares fit; dotted lines bracket the standard

Appendix 3

Quality Control

The work described in this report is directed towards a method which would apply accurate analysis to an undefined atmospheric enviroment. Thus, it is a quality control effort. Within this project, quality control is maintained by the following procedures:

1. The various pieces of equipment used (Philips AXS and APD, Beckman 603 Atomic Absorption units, Spex ICP) are maintained by factory representatives with a maintenance log recorded. Instruments were always used according to manufcturer's directions.

2. Chemicals and solvents were used within reasonable expiration dates. The multiplicity of analyses--XRF, AA, ICP--would be likely to reveal any impurity of significance.

3. Replicate sampling techniques were used whenever feasible; XRF standards were mostly in triplicate, a few in duplicate.

4. No difficulties with collection efficiency (breakthrough) or sample stability were observed.

5. Spiked filters were analyzed by AA along with the fume samples. Per cent recoveries were always completely adequate (usually less than 5%). AA standard calibration curves were linear with a correlation coefficient of 0.99 or better.

6. The glassware was always cleaned according to the procedure described in reference 16 or equivalent.

7. No NBS (or equivalent) welding fume samples are available. The alternative method chosen to ensure accuracy was to have two independent analytical methods for comparison to the XRF results, viz., atomic absorption and ICP. The data substantiate the applicability of this scheme.

DOCUMENTATION PAGE	1. REPORT NO. NA	2. NA	3. Recipient's Accession No. NA PB87 116907
4. Title and Subtitle: Feasibility Study of X-Ray Fluorescence for Analysis of Welding and Brazing Fumes			5. Report Date: NA
			6. U288413
7. Author(s): Carsey, T. P.			8. Performing Organization Rept. No. NA
9. Performing Organization Name and Address: Industrial Hygiene Section, Industry-wide Studies Branch, Division of Surveillance, Hazard Evaluation and Field Studies, NIOSH, Cincinnati, Ohio			10. Project/Task/Work Unit No. NA 11. Contract(C) or Grant(G) No. (C) (G) NA
12. Sponsoring Organization Name and Address: Same as Above			13. Type of Report & Period Covered: Industry-wide Studies 14. NA

15. Supplementary Notes

NA

16. Abstract (Limit: 200 words)

An X-ray fluorescence technique (XRF) was developed for the analysis of welding and brazing fumes. Welding or brazing fumes were collected on six standard filter cassettes and examined by electronmicroscopy and X-ray diffraction to assess the particle size and deposition. Samples were then analyzed by XRF, ashed, and analyzed by atomic absorption (AA). Samples were also analyzed by inductively coupled argon plasma emission spectroscopy (ICP). An XRF standardization method was developed using laboratory generated fume samples. Field samples were obtained at three welding shops, and samples were analyzed by XRF, AA and ICP. Results between the three methods were in good agreement. The author concludes that the XRF technique is suitable for fume analysis, although a more adequate standardization procedure is needed.

17. Document Analysis a. Descriptors

Methodology, Analytical-instrumentation, Diagnostic-techniques, Sample-preparation, Chemical-analysis, Chemical-properties, Physical-properties

b. Identifiers/Open-Ended Terms

c. COSATI Field/Group

18. Availability Statement	19. Security Class (This Report)	21. No. of Pages
Available to the Public	NA	65
	20. Security Class (This Page)	22. Price

(ANSI-Z39.18) See Instructions on Reverse OPTIONAL FORM 272 (4-77) (Formerly NTIS-35) Department of Commerce